UNIVERSITÀ DEGLI STUDI DI PADOVA

Università degli Studi di Padova
Université de Cergy-Pontoise

Master of Civil Engineering

THE INFLUENCE OF AGGREGATES ON THE MECHANICAL CHARACTERISTICS OF MORTARS EXPOSED TO HIGH TEMPERATURES

Master Thesis By:

Dounia **SLIKA**

Supervisors:

Carlo **PELLEGRINO**

Anne-Lise **BEAUCOUR**

Rijaniaina **NIRY RAZAFINJATO**

Academic year: **2015**

Acknowledgments

Foremost, I would like to express my sincere gratitude to my advisors Mr. Carlo Pellegrino, Mr. Rijaniaina NIRY RAZAFINJATO and Mrs. Anne-Lise BEAUCOUR for the continuous support of my study and research, for their patience, motivation, enthusiasm, and immense knowledge. Their guidance helped me in all the time of research and writing of this thesis. I could not have imagined having a better advisors and mentors for my study.
I am using this opportunity to express my gratitude to everyone who supported me throughout the course of this master project. I am thankful for their aspiring guidance, invaluably constructive criticism and friendly advice during the project work. I am sincerely grateful to them for sharing their truthful and illuminating views on a number of issues related to the project. I express gratitude to all of the Department faculty members for their help and support. I also thank my parents for the encouragement, support and attention.

Summary

List of figures

List of tables

Abstract

Concretes containing mineral admixtures are used extensively throughout the world for their good performance and for ecological and economic reason. In many modern engineering problems concrete results exposed to temperature ranges over ambient conditions (higher than 50°C), as when it takes part of industrial installations (pressure furnaces, chimneys, nuclear reactors), or in accidental situations like explosions or Fire. The stability of concrete at high temperatures is of great interest in safety evaluation in civil constructions. Because of an increased occurrence of tunnel fires, many European programs have been established in order to study fire behavior of concrete.

In this experimental investigation, the effect of elevated temperatures on the physical and mechanical properties of concrete mixtures produced by different types of sands are extensively examined.
It is studied the behavior of mortars prepared with three different sands: granite sand (SG), black limestone sand (SN) and flint sand (SX).

The study is divided into three parts:

1. the first part is dedicated to the determination of the characteristics of the sands used, then the correct mixing of mortars is determined. The three mortars and cement paste both ordinary and high-performance are packed.
2. In the second part is analyzed the behavior at high temperatures of mortars through dilatometer test method and ATG-DSC test.
3. The last part is dedicated to results and comments.

The final objective is to characterize in the best way the concrete exposed to high temperatures, such as in case of fire.

Introduction

The mechanical properties such as strength, modulus of elasticity and volume stability of concrete are significantly reduced during accidental situations like explosions or fire. This may result in undesirable structural failures. Therefore, the properties of concrete retained after a fire are of still importance for determining the load carrying capacity and for reinstating fire-damaged constructions. When exposed to high temperature, the chemical composition and physical structure of the concrete change considerably. The dehydration such as the release of chemically bound water from the calcium silicate hydrate (CSH) becomes significant above about 110 °C. The dehydration of the hydrated calcium silicate and the thermal expansion of the aggregate increase internal stresses and from 300 °C micro-cracks are induced through the material. Calcium hydroxide [$Ca(OH)_2$], which is one of the most important compounds in cement paste, dissociates at around 530 °C resulting in the shrinkage of concrete. The fire is generally extinguished by water and CaO turns into [$Ca(OH)_2$] causing cracking and crumbling of concrete. Therefore, the effects of high temperatures are generally visible in the form of surface cracking and spalling. Some changes incolour may also occur during the exposure. The alterations produced by high temperatures are more evident when the temperature surpasses 500 °C. Most changes experienced by concrete at this temperature level are considered irreversible. CSH gel, which is the strength giving compound of cement paste, decomposes further above 600 °C. At 800 °C, concrete is usually crumbled and above 1150 °C feldspar melts and the other minerals of the cement paste turn into a glass phase. As a result, severe micro-structural changes are induced and concrete loses its strength and durability.
Concrete is a composite material produced from aggregate, cement, and water. Therefore, the type and properties of aggregate also play an important role on the properties of concrete exposed to elevated temperatures. The strength degradations of concretes with different aggregates are not same under high temperatures. This is attributed to the mineral structure of the aggregates. Quartz in siliceous aggregates polymorphically changes at 570 °C with a volume expansion and consequent damage. In limestone aggregate concrete, $CaCO_3$ turns into CaO at 800–900 °C, and expands with temperature. Shrinkage may also start due to the decomposition of $CaCO_3$ into CO_2 and CaO with volume changes causing destructions. Consequently, elevated temperatures and fire may cause aesthetic and functional deteriorations to the buildings.

Chapter I: Experimental protocol

I.1. Presentation of materials

Concrete is an important and useful material: concrete is the backbone of the world's infrastructure, used in vast amounts to make roads, buildings, bridges, and other structures. Concrete is a complex material which behaves in an appropriately complex manner. Its properties vary with age, temperature and humidity. The concrete is a composite material having high heterogeneity consists of a mixture of aggregates, a cement paste optionally incorporating additives. Cement is the binder component of concrete, the glue that holds the filler together to create a uniform, strong material. The filler in concrete consists primarily of aggregate particles. These can be made out of lots of different materials, but the vast majority of aggregate is just sand, gravel, and rocks, which are cheap, plentiful, and easily obtained from nature. Cement, on the other hand, is a man-made material that requires high-temperature processing, grinding, and other costly and energy-intensive steps. The concrete can also be considered as a multiphase material containing three phases: solid (aggregates and cement paste), liquid (free and adsorbed water) and gas (air and steam). Its mechanical properties develop through the hydration of cement. The complexity of its microstructure is a cause of its special mechanical behavior when subjected to various stresses (heat, water, mechanical, chemical, etc..). It is therefore necessary to know the most of this microstructure and behavior of each of these phases in order to understand more effectively then, on the macroscopic scale, the response of concrete withstand the forces that can undergo.

Figure 1 : the basic ingredients of concrete.

From left to right: fine aggregate (sand), coarse aggregate, water, and cement

I.1.1.Aggregates

a) Mineral composition

Aggregates occupy a large part of the concrete volume (60-75%) and are the source of its strength. It is an inert material in ambient temperature (unless pathological conditions, ex. alkali-aggregate reaction). The aggregates used should have good mechanical strength and their granulometric curve should be optimized in order to fulfill as much as possible of voids in the concrete. This is why several granular classes in the same concrete is used which is sand, gravel. Aggregates are generally of natural origin. They come mainly from siliceous and calcareous sedimentary rocks, metamorphic rocks such as quartzite, or magmatic rocks such as basalt, granite or porphyry. Regardless of their nature, can be alluvial aggregates (called aggregates rolled) or career (so crushed aggregate). The origin of the aggregates can also be artificial (of mineral origin, processed, expanded shale or slag aggregates) or after recycling (crushed concrete ...).
To obtain concrete with good characteristics, several parameters are involved in the choice of aggregates such as quality (mechanical, physical-chemical, cleanliness and so on), mineralogy, form aggregates and a suitable granulometry associated.
In this paper we consider three natural aggregates: black limestone, granite and flint.

- Granite

Granite is a common type of felsic intrusive igneous rock that is granular and phaneritic in texture. These rocks mainly consist of feldspar, quartz, mica, and amphibole minerals, which form interlocking, somewhat equigranular matrix of feldspar and quartz with scattered darker biotite mica and amphibole (often hornblende) peppering the lighter color minerals. Occasionally some individual crystals (phenocrysts) are larger than the groundmass, in which case the texture is known as porphyritic. A granitic rock with a porphyritic texture is known as a granite porphyry. Granites can be predominantly white, pink, red or gray in color, depending on their mineralogy. It is the potassium feldspar that gives many granites a distinctive pink color. The extrusive igneous rock equivalent of granite is rhyolite.
Chemical composition:

- SiO_2 (silica) 72.04 %
- Al_2O_3 (alumina) 14.42 %
- K_2O 4.12 %
- Na_2O 3.69 %
- CaO 1.82 %
- FeO 1.68 %
- Fe_2O_3 1.22 %
- MgO 0.71 %
- TiO_2 0.30 %
- P_2O_5 0.12 %
- MnO 0.05 %

By definition, granite is an igneous rock with at least 20% quartz and up to 65% alkali feldspar by volume.
Quartz is the second most abundant mineral in the earth's continental crust, it is made up of a continuous framework of SiO_4 silicon–oxygen tetrahedra, with each oxygen being shared between two tetrahedra, giving an overall formula SiO_2. Quartz belongs to the trigonal crystal system. The ideal crystal shape is a six-sided prism terminating with six-sided pyramids at each end. In nature quartz crystals are often twinned, distorted, or so intergrown with adjacent crystals of quartz or other minerals as to only show part of this shape, or to lack obvious crystal faces altogether and appear massive. Well-formed crystals typically form in a 'bed' that has unconstrained growth into a void; usually the crystals are attached at the other end to a matrix and only one termination pyramid is present. However doubly-terminated crystals do occur where they develop freely without attachment, for instance within gypsum. A quartz geode is such a situation where the void is approximately spherical in shape, lined with a bed of crystals pointing inward.
α-quartz crystallizes in the trigonal crystal system. β-quartz belongs to the hexagonal system. Both α-quartz and β-quartz are examples of chiral crystal structures composed of achiral building blocks (SiO_4 tetrahedra). The transformation between α- and β-quartz at 573°C involves a comparatively minor rotation of the tetrahedra with respect to one another, without change in the way they are linked.
The micas is another minerals found in granite aggregates.
The micas group of sheet silicate (phyllosilicate) minerals includes several closely related materials having nearly perfect basal cleavage. All are monoclinic, with a tendency towards pseudohexagonal crystals, and are similar in chemical composition. The nearly perfect cleavage, which is the most prominent characteristic of mica, is explained by the hexagonal sheet-like arrangement of its atoms.
The word mica is derived from the Latin word mica, meaning a crumb, and probably influenced by micare, to glitter.

Chemically, micas can be given the general formula:

$$X_2Y_{4-6}Z_8O_{20}(OH,F)_4$$

in which:

X is K, Na, or Ca or less commonly Ba, Rb, or Cs;
Y is Al, Mg, or Fe or less commonly Mn, Cr, Ti, Li, etc.;
Z is chiefly Si or Al, but also may include Fe^{3+} or Ti.

Structurally, micas can be classed as dioctahedral (Y = 4) and trioctahedral (Y = 6). In the first class we find white micas $(XY^{3+})_2\ [AlSi_3O_{10}(OH,F)_2]^{7-}$, rich in potassium and aluminum, the most known is the muscovite $(K^+\ Al^{3+})_2\ [AlSi_3O_{10}(OH,F)_2]^{7-}$. In the second class we can find black containing magnesium and potassium $XY^{2+}_3\ [Al_{1+x}Si_{3-x}O_{10}(OH)_2]^{7-}$. In black mica group is located biotite, whose empirical formula is $K^+(Mg, Fe,Ti)^{2+}_3[Al_{1+x}Si_{3-x}O_{10}(OH)_2]^{7-}$.

- Black limestone

Like most other sedimentary rocks, most limestone is composed of grains. Most grains in limestone are skeletal fragments of marine organisms such as coral or foraminifera. Other carbonate grains comprising limestones are ooids, peloids, intraclasts, and extraclasts. These organisms secrete shells made of aragonite or calcite, and leave these shells behind after the organisms die.
Limestone often contains variable amounts of silica in the form of chert (chalcedony, flint, jasper, etc.) or siliceous skeletal fragment (sponge spicules, diatoms, radiolarians), and varying amounts of clay, silt and sand (terrestrial detritus) carried in by rivers.
Black limestone is a variety of limestone and belongs to the category of sedimentary rocks.

- Flint

Flint is a hard, sedimentary cryptocrystalline form of the mineral quartz, categorized as a variety of chert. It occurs chiefly as nodules and masses in sedimentary rocks, such as chalks and limestones. Inside the nodule, flint is usually dark grey, black, green, white or brown in colour, and often has a glassy or waxy appearance. A thin layer on the outside of the nodules is usually different in colour, typically white and rough in texture. From a petrological point of view, "flint" refers specifically to the form of chert which occurs in chalk or marly limestone.

b) Physical properties

- Determination of the density and water absorption according to EN 1097-6

1. fill with water the pycnometer, close it and weigh (M3)
2. place the sample in a pycnometer and fill with water until the entire specimen is submerged
3. The specimen is immersed in the solution for 48 hours to guarantee it is completely saturated (M2)
4. the surface specimen is dried and it is stirred often to ensure homogeneous drying so that only the pores still contain water and then weigh to obtain the saturated surface dry mass (M1)
5. progress with prolonged drying in an oven (48h) to remove any pore water aggregates then weigh to obtain the dry mass (M4)

The particle densities (ρ_a, ρ_{rd}, ρ_{ssd}), in mega grams per cubic meter, and the water absorption ratio are determined according to the following equations:

$$\rho_a = \frac{M_4}{M_4 - (M_2 - M_3)}$$ relative particle density

$$\rho_{rd} = \frac{M_4}{M_1 - (M_2 - M_3)}$$ saturated surface-dry density

$WA_{24} = \frac{100 \cdot (M1 - M4)}{M4}$ water absorption (as percentage of dry mass) after immersion for 24 hours

The results obtained for the three sands are the following

	Density [Mg/m^3]	water absorption W_{24} [%]
Black limestone	2450	0.49
Granite	2680	0.45
Flint	2780	1.04

- Granulometry curves

The curve which shows the distribution of grains with certain sizes in an aggregate, is called Granulometry Curve. In order to determine optimal amounts of the sands to be included in the realization of the mortars we must realize sands granulometry curves.
Granulometry curve is determined with sieve analysis. The method for performing sieve analysis test on an aggregate pile is specified in EN 933-1.

Methods for sampling:

The objective of sampling is to obtain a bulk sample that is representative of the average properties of the batch, it is important to remember that information obtained from test samples is only as representative of the material as the samples on which the tests are undertaken. Bulk samples can be reduced to sample sizes suitable for testing by using a riffle box.
There are several sizes of riffle box to suit different sizes of aggregate, one of which is illustrated in figure. The box consists of an even number of chutes discharging in alternate directions.
The material is passed through the riffle box, which divides it into two portions, one of which is discarded. The other portion is passed through again and the process repeated until the sample has been reduced to the required size. It should be noted that a riffle box can only be used on dry material.

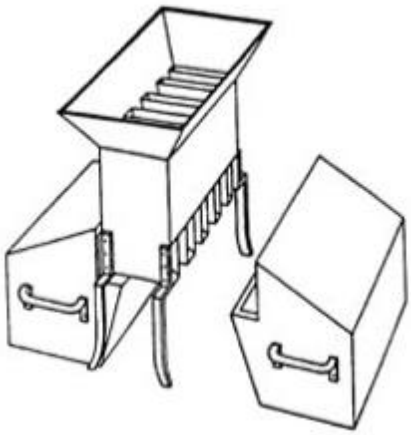

Figure 2: riffle box

Determination of Particle Size Distribution -Sieving Method (EN 933-1):

In a sieve analysis, a sample of dry aggregate of known weight is separated through a series of sieves with progressively smaller openings. Once separated, the weight of particles retained on each sieve is measured and compared to the total sample weight.
Particle size distribution is then expressed as a percent retained by weight on each sieve size. Results are usually expressed in tabular or graphical format.
The test consists of dividing up and separating, by means of series of sieves, a material into several particle size classification of decreasing sizes. The aperture sizes and the number of sieves are selected in accordance with the nature of the sample and the accuracy required.
The mass of the particles retained on the various sieves is related to the initial mass of the material.
The cumulative percentages passing each sieve are reported in numerical form and in graphical form.

Modus Operandi: Granulometry

1. Wash the material to remove impurities

Figure 3: washing the material with water

2. dry the aggregate in an oven for 48 hours at 105 ° C

Figure 4: oven at 105°C

3. Pour the washed and dried material into sieving column. The column comprises a number of sieves fitted together and arranged, from top to bottom, in order of decreasing aperture sizes with pan and lid (4mm, 2mm, 1mm, 0.5mm, 0.25 mm, 0.125mm, 0.063mm).

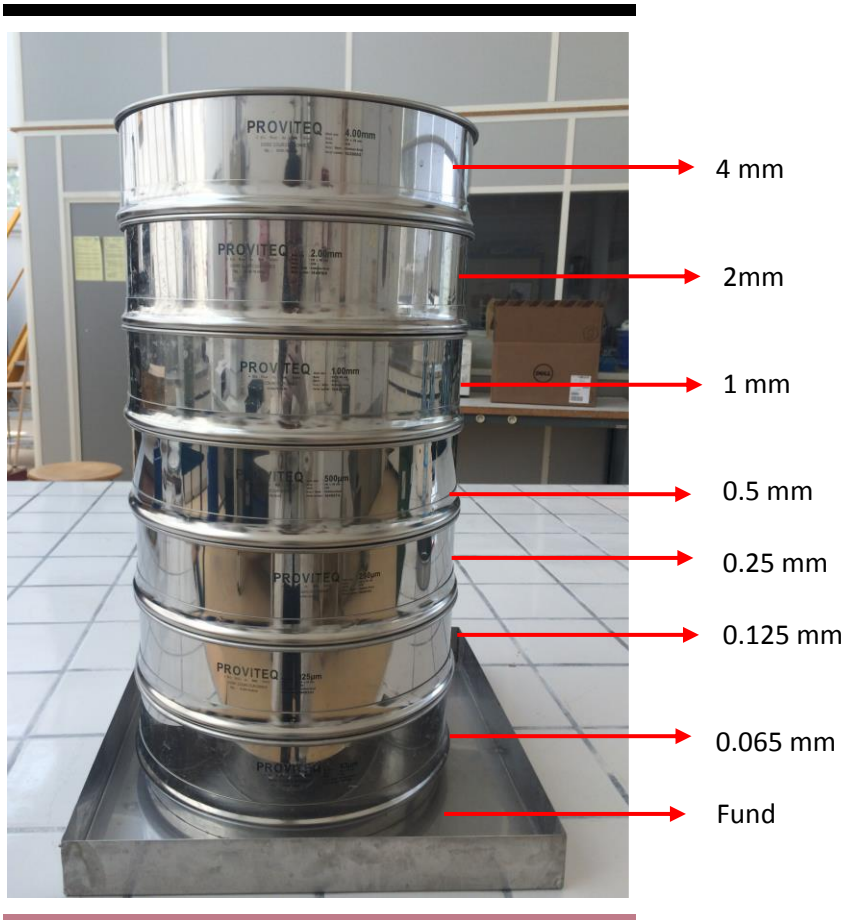

Figure 5: the column of sieves

4. Shake the column, manually or mechanically, then remove the sieves one by one, and shake each sieve manually ensuring no material is lost.
5. Transfer all the material, which passes each sieve onto the next sieve in the column before continuing the operation with that sieve.
6. Weigh the retained material for the sieve with the largest aperture and record its mass, Carry out the same operation for all the sieves.
7. Record the various masses on test data sheet as mass of material retained.
8. Calculate the mass retained on each sieve as percentage of the original dry mass M
9. Calculate the cumulative percentage of the original dry mass passing each sieve down
10. If the sum of the masses retained differs more than 1% from the mass M, the test shall be repeated.

Below are shown the results for each aggregate:

Table 1: granulometry

	silex				
sieve [mm]	refusal [g]	cumulative refusal Ri [g]	refusal [%]	cumulative refusal [%]	tamisat cumulative [%]
4	2,00	2,00	0,64	0,64	99,36
2	24,00	26,00	7,69	8,33	91,67
1	24,00	50,00	7,69	16,03	83,97
0,5	40,00	90,00	12,82	28,85	71,15
0,25	126,00	216,00	40,38	69,23	30,77
0,125	74,00	290,00	23,72	92,95	7,05
0,063	20,00	310,00	6,41	99,36	0,64
fund	2,00	312,00	0,64	100,00	0,00
refusal weight [g]		312,00	100,00	100,00	
initial weight [g]		318,00			
loss [g]		6,00			
loss [%]		1,886792			

	calcaire noire				
sieve [mm]	refusal [g]	cumulative refusal Ri [g]	refusal [%]	cumulative refusal [%]	tamisat cumulative [%]
4	10,00	10,00	3,14	3,14	96,86
2	82,00	92,00	25,79	28,93	71,07
1	100,00	192,00	31,45	60,38	39,62
0,5	60,00	252,00	18,87	79,25	20,75
0,25	34,00	286,00	10,69	89,94	10,06
0,125	20,00	306,00	6,29	96,23	3,77
0,063	12,00	318,00	3,77	100,00	0,00
fund	0,00	318,00	0,00	100,00	0,00
refusal weight [g]		318,00	100,00	100,00	
initial weight [g]					
loss [g]					
loss [%]					

	granite				
sieve [mm]	refusal [g]	cumulative refusal Ri [g]	refusal [%]	cumulative refusal [%]	tamisat cumulative [%]
4	20,00	20,00	6,29	6,29	93,71
2	138,00	158,00	43,40	49,69	50,31
1	66,00	224,00	20,75	70,44	29,56
0,5	42,00	266,00	13,21	83,65	16,35
0,25	26,00	292,00	8,18	91,82	8,18
0,125	14,00	306,00	4,40	96,23	3,77
0,063	10,00	316,00	3,14	99,37	0,63
fund	2,00	318,00	0,63	100,00	0,00
refusal weight [g]		318,00	100,00	100,00	
initial weight [g]					
loss [g]					
loss [%]					

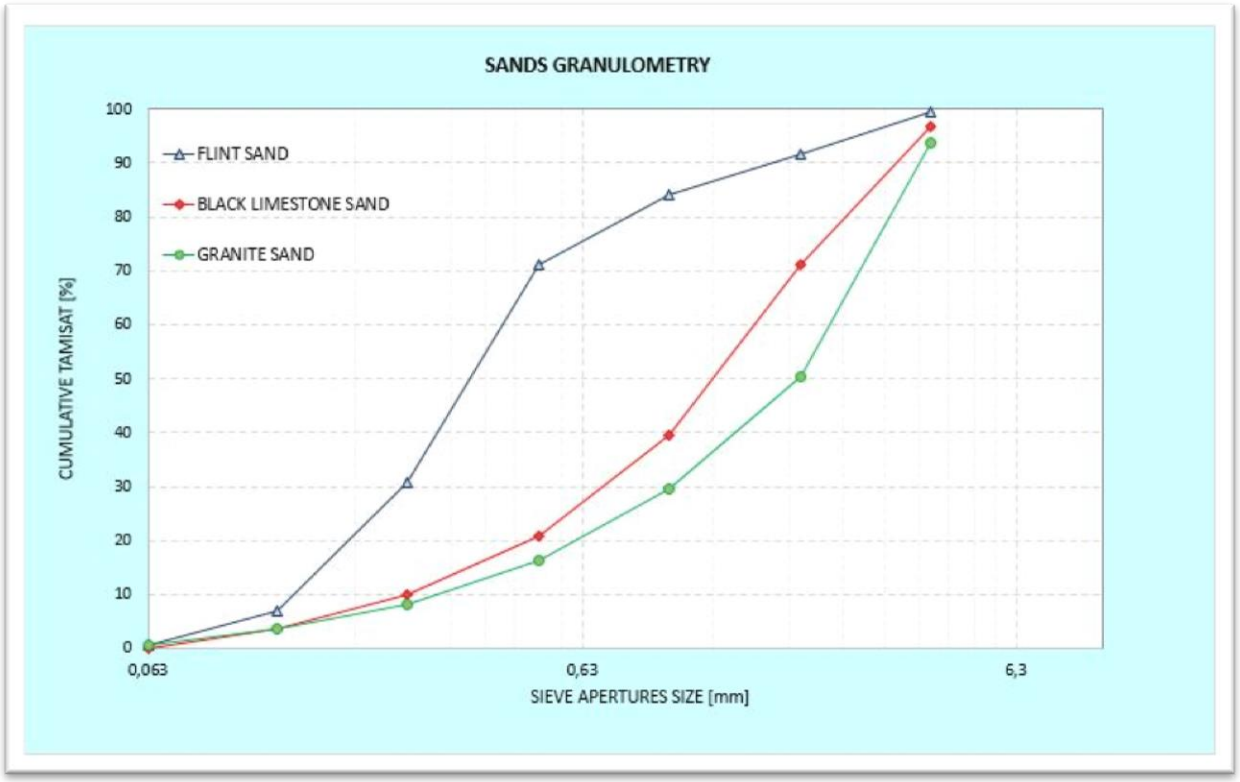

Figure 6: particle's size distribution curve

Analyzing the graph you can see immediately that the curve of the granite is very smooth, without spikes; this means regularity of the statistical distribution of the diameters of this sand.
We can also see that granite sand is the most coarse, while flint sand is more fine. We can better understand this statement analyzing the characteristic diameter for each sand (D50):

- Flint D50 = 0.375 mm
- Black limestone D50 = 1.33mm
- Granite D50 = 2 mm

All this information is necessary for mortars formulation and realization.

I.1.2. Mortar and cement paste

a) Cement paste

The cement paste is 25 to 40% of the total volume of the concrete. Is the dough that ensures the role of matrix in the concrete binder aggregates. It is formed by the mixing of cement and water. The generally used in civil engineering is the cement "Portland" cement is a hydraulic binder, that is to say capable of setting and hardening with water.
The cement consists essentially of the following types of mineralogical constituents:

Table 2: mineralogical constituents of cement

Chemical Name	Chemical Formula	Oxide Formula	Cement Notation	Mineral Name
Tricalcium Silicate	Ca_3SiO_5	$3CaO.SiO_2$	C_3S	Alite
Dicalcium Silicate	Ca_2SiO_4	$2CaO.SiO_2$	C_2S	Belite
Tricalcium Aluminate	$Ca_3Al_2O_6$	$3CaO.Al_2O_3$	C_3A	Aluminate
Tetracalcium Aluminoferrite	Ca_2AlFeO_5	$4CaO.Al_2O_3.Fe_2O_3$	C_4AF	Ferrite
Calcium hydroxide	$Ca(OH)_2$	$CaO.H_2O$	CH	Portlandite
Calcium sulfate dihydrate	$CaSO_4.2H_2O$	$CaO.SO_3.2H_2O$	$C\overline{S}H_2$	Gypsum
Calcium oxide	CaO	CaO	C	Lime

About 90-95% of a Portland cement is comprised of the four main cement minerals, which are C_3S, C_2S, C_3A, and C_4AF, with the remainder consisting of calcium sulfate, alkali sulfates, unreacted (free) CaO, MgO, and other minor constituents left over from the clinkering and grinding steps. The four cement minerals play very different roles in the hydration process that converts the dry cement into hardened cement paste. The C_3S and the C2S contribute virtually all of the beneficial properties by generating the main hydration product, C-S-H gel. However, the C3S hydrates much more quickly than the C_2S and thus is responsible for the early strength development. The C_3A and C_4AF minerals also hydrate, but the products that are formed contribute little to the properties of the cement paste.

Tricalcium Silicate $3CaO, SiO_2$ (C_3S) 60-65 %

C_3S is the most abundant mineral in portland cement, and it is also the most important. The hydration of C_3S gives cement paste most of its strength, particularly at early times.
Pure C_3S can form with three different crystal structures. At temperatures below 980˚C the equilibrium structure is triclinic. At temperatures between 980˚C – 1070˚C the structure is monoclinic, and above 1070˚C it is rhombohedral. In addition, the triclinic and monoclinic structures each have three polymorphs, so there are a total of seven possible structures. However, all of these structures are rather similar and there are no significant differences in the reactivity. The most important feature of the structure is an awkward and asymmetric packing of the calcium and oxygen ions that leaves large “holes” in the crystal lattice. Essentially, the ions do not fit together very well, causing the crystal structure to have a high internal energy. As a result, C3S is highly reactive.

The C_3S that forms in a cement clinker contains about 3-4% of oxides other than CaO and SiO_2. Strictly speaking, this mineral should therefore be called alite rather than C_3S. In a typical clinker the C_3S would contain about 1 wt% each of MgO, Al_2O_3, and Fe_2O_3, along with much smaller amounts of Na_2O, K_2O, P_2O_5, and SO_3. These amounts can vary considerably with the composition of the raw materials used to make the cement.

Dicalcium Silicate	$2CaO, SiO_2$	(C_2S)	20-25 %

As with C_3S, C_2S can form with a variety of different structures. There is a high temperature a structure with three polymorphs, a b structure in that is in equilibrium at intermediate temperatures, and a low temperature g structure. An important aspect of C2S is that g-C_2S has a very stable crystal structure that is completely unreactive in water. Fortunately, the b structure is easily stabilized by the other oxide components of the clinker and thus the g form is never present in portland cement. The crystal structure of b-C2S is irregular, but considerably less so than that of C_3S, and this accounts for the lower reactivity of C_2S. The C_2S in cement contains slightly higher levels of impurities than C_3S.

Tricalcium Aluminate	$3CaO, Al_2O3$	(C_3A)	8-12 %

Tricalcium aluminate (C_3A) like C_3S, it is highly reactive, releasing a significant amount of exothermic heat during the early hydration period. Unfortunately, the hydration products of formed from C_3A contribute little to the strength or other engineering properties of cement paste. In certain environmental conditions (i.e., the presence of sulfate ions), C_3A and its products can actually harm the concrete by participating in expansive reactions that lead to stress and cracking.

Tetracalcium Aluminoferrite	$4CaO, Al_2O_3, Fe_2O_3$	(C_4AF)	8-10 %

A stable compound with any composition between C_2A and C_2F can be formed, and the cement mineral termed C_4AF is an approximation that simply the represents the midpoint of this compositional series. The crystal structure is complex, and is believed to be related to that of the mineral perovskite. The actual composition of C_4AF in cement clinker is generally higher in aluminum than in iron, and there is considerable substitution of SiO2 and MgO. However, the composition will vary somewhat depending on the overall composition of the cement clinker.

When adding water to the cement, the hydration reactions are triggered causing the formation of a porous network and the formation of hydrated products. The main hydrates formed are the Calcium-Silicate-Hydrate (C-S-H), calcium hydroxide $Ca(OH)_2$, the calcium-aluminates-Hydrate.

The C-S-H gel is not only the most abundant reaction product, occupying about 50% of the paste volume, but it is also responsible for most of the engineering properties of cement paste. This is not because it is an intrinsically strong or stable phase but because it forms a continuous layer that binds together the original cement particles into a cohesive whole. All the other hydration products form as discrete crystals that are intrinsically strong but do not form strong connections to the solid phases they are in contact with and so cannot

contribute much to the overall strength. The ability of the C-S-H gel to act as a binding phase arises from its nanometer-level structure.

Calcium hydroxide, also known by its mineral name portlandite, contributes slightly to the strength and impermeability of the paste, because it reduces the total pore volume by converting some of the liquid water into solid form. In this respect it is much less important than the C-S-H, however. CH is the most soluble of the hydration products, and thus is a weak link in cement and concrete from a durability point of view. If the paste is exposed to fresh water, the CH will leach out (dissolve), increasing the porosity and thus making the paste more vulnerable to further leaching and chemical attack.
Calcium hydroxide is believed to play a role in limiting the amount of shrinkage that occurs when a cement paste is dried. As water is removed from the pore system, the C-S-H gel phase collapses causing an overall shrinkage, while other crystalline phases such as CH are unaffected. As the C-S-H starts to shrink the CH that is in contact with it acts as a restraint, so that the overall shrinkage is less than it would be if the CH were not present.

In any composite material the physical and chemical properties of the constituents and the interactions between them determine the behavior of the material. Concrete is a composite material with coarse and fine aggregate embedded in a cement paste matrix. Thus the mechanical behavior and the durability of the concrete is affected by both the aggregate and the cement paste as well as the interfacial zone between them. For concrete to perform satisfactorily it is essential that the interfacial zone be as dense as possible, giving a good bond between the aggregate and the matrix.
With respect to the interaction between matrix and aggregate of concrete there are three mechanisms to be considered:

- Physical interaction

For aggregates with well-polished mineral surfaces (e.g. quartz) and no chemical interaction with the matrix, the bond strength may be negligible even if the matrix is strong. The aggregate - matrix interface becomes the weakest link in the system.

- Physical-chemical interaction

For aggregates having a chemical interaction with the cement paste matrix (e.g. car- bonate rocks), there is evidence that a strong chemical bond between the aggregate and the cement paste matrix may developed.

- Mechanical interlocking

For porous aggregates or aggregates with a rough surface, the cement paste or cement hydration products may penetrate into cavities or large pores on the aggregate surface.
These act as multiple "hooks" binding the aggregate and the matrix together.

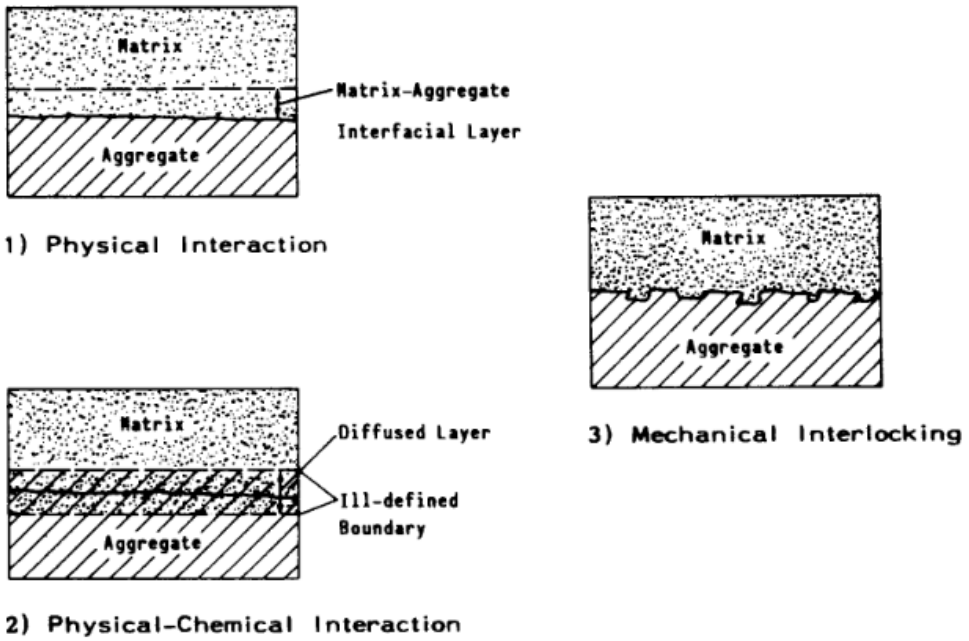

Figure 7: schematic presentation of the interfacial zone between cement paste matrix and aggregate

Concrete is made up of two distinctly different constituents, the cement paste and the aggregate, and there is a tendency to assume that the properties of each of these is unaffected by the presence of the other. The cement paste can affect the aggregate by causing a chemical reaction between the highly alkaline pore solutions and reactive silica in the aggregate. The presence of the aggregate also affects the cement paste. The cement particles in fresh concrete, which are suspended in the mix water, cannot pack together as efficiently when they are in the close vicinity of a much larger solid object, such an aggregate particle. This is actually a general phenomenon associated with particle packing, known as the "wall effect." In the case of concrete, this is effect is magnified by the shearing stresses exerted on the cement paste by the aggregate particles during mixing, which tend to cause the water to separate from the cement particles. The result is a narrow region around the aggregate particles with fewer cement particles, and thus more water. This is called the interfacial transition zone, abbreviated ITZ. A recent review of the microstructure of the rock aggregate-cement paste interface and its effect on the mechanical behavior of the concrete has been given by Diamond. The principal features of the transition zone between rock aggregate and cement paste are shown in figure:

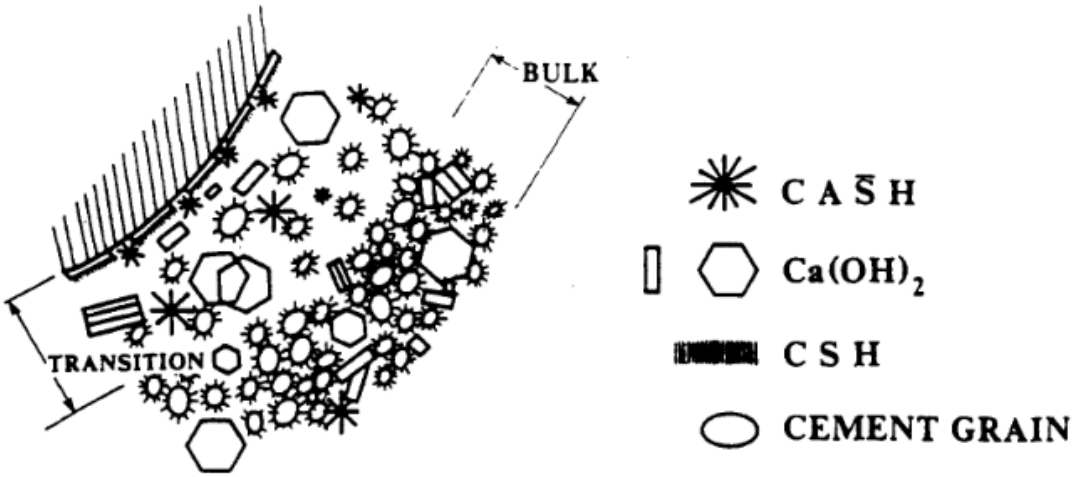

Figure 8: schematic presentation of the microstructure of the transition zone between polished rock aggregate and cement paste

The ITZ is a region with a higher w/c, and thus a higher porosity, than the bulk paste. It is not uniform, but varies from point to point along each aggregate particle. Because of the larger pores, the ITZ is characterized by the presence of larger crystals, particularly of calcium hydroxide, than are found in the bulk paste. The ITZ tends to be larger around larger aggregate particles. The ITZ has important effects on the properties of concrete, because it tends to act as the "weak link in the chain" when compared to the bulk cement paste and the aggregate particles. Thus the lower strength and stiffness of the ITZ translate directly into lower strength and stiffness values for concrete as compared to cement paste. The total volume of ITZ in a concrete increases with the total amount of large aggregate and with the average size of the aggregate, which explains why the strength is observed to decrease with both of these parameters. The ITZ is also more permeable than the bulk paste, due to its higher porosity. In most concretes the ITZs are linked (percolated), creating a continuous high-permeability phase across the structure. As a result, the permeability of concrete can be greater than that of the pure cement paste it contains. The durability of concrete is inversely related to the permeability, as most damage mechanisms involve the diffusion of reactive ions into the concrete to attack either the cement paste or the steel reinforcement.

b) Formulation (concrete mixture)

The physical properties of density and strength of concrete are determined, in part, by the proportions of the three key ingredients, water, cement, and aggregate. You have your choice of proportioning ingredients by volume or by weight.

The use of the Dreux-Gorisse method in the preparation of concrete mixture

It is a very practical and simplified method, it depend generally on granular curves of references, the tables and abacuses established from the practical observation. Some morphological and petrophysical properties of the aggregates must be known initially, it is fixed, then; the average proprieties of the concrete to be formulated, in particular its consistency and its mechanical strength to compression at 28 days.
The method consisting by the following stages:

- Proportioning of the cement/water ratio (C/W)
- determination of the cement content
- determination of the aggregates content
- determination of the compactness of concrete

The aim of this work is to analyze the influence of the aggregates on concrete properties at high temperatures, we need to reduce the granular skeleton in its simplest form, which is composed only by sand. The set of specimens will be composed solely of water, cement and aggregates (mortal).

1. Cement content

The cement content differs from the aggregates content. The cement/water ratio (C/W) is approximately evaluated using the overage strength σ_{28} and the required plasticity through the following formula.

$$\sigma_{28} = G \cdot \sigma_c \cdot (\frac{C}{W - 0.5})$$

where

σ_{28} : is the required overage compressive strength at 28 days
σc : is the true cement class at 28 days
C: is then cement content (expressed in kg / m^3)
W: is the total water content in dry materials (expressed in kg / m^3)
G: is the granular coefficient with values are given in table according to the aggregates quality and dimensions.

Table 3: approximate values of the granular coefficient G

aggregates quality	Aggregates dimension D		
	fine: D≤16 mm	medium: 25≤D≤40mm	coarse: D≥63 mm
very good	0.55	0.6	0.65
good, common	0.45	0.5	0.55
fairly good	0.35	0.4	0.45

Knowing the report C/W ratio and the desired workability, considered as a basic data, the cement content can be approximately evaluated by using the chart (Dreux, 1981) depicted in Figure.

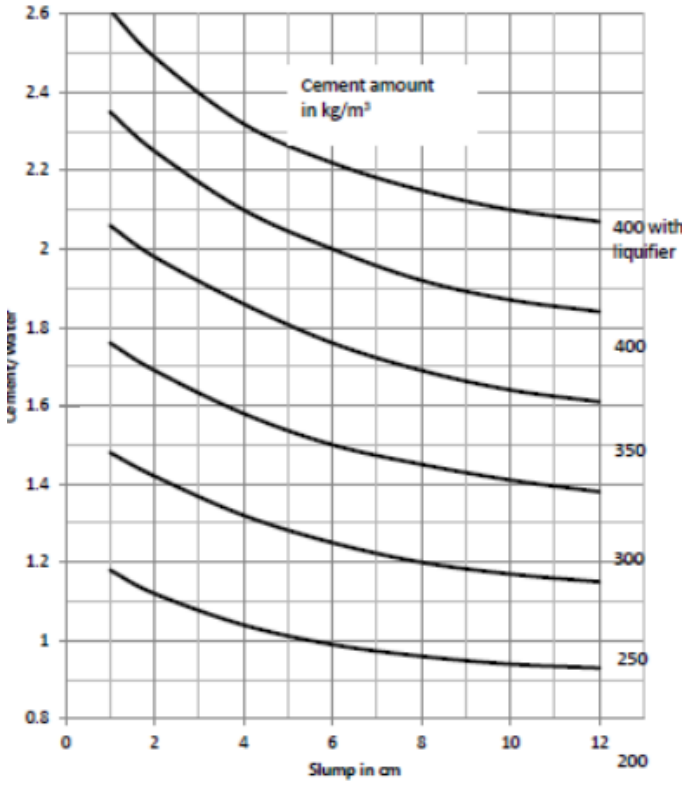

Figure 9: Chart giving approximate cement content to use in respect to the required C/W ratio and the workability (cone collapse)

2. Water content

The choice of the cement content C and the C/W ratio values lead obviously to water content which value is only approximate.
Measuring water content of the sand will be made 30 minutes before mixing in order to have the most accurate water correction possible.

Sands/Cement ratio will be kept constant relative to the reference concrete and the mixing water will be correct from the water provided by the sands.

3. Calculation method

C_M [m^3] : ciment mortar volume

S_M [m^3] : sand mortar volume

W_M [m^3] : water mortar volume

C_c [m^3] : ciment concrete volume

S_c [m^3] : sand concrete volume

W_c [m^3] : water concrete volume

Compactness [volume] for 1 m^3

- $C_M + S_M + W_M = 1\ m^3$

conditions imposed

- $W_M = W_C$
- $\frac{S_c}{C_c} = \frac{S_m}{C_m}$ = Cost

the concrete cement dosage C_c is taken to 360 kg/m^3 :

$C_M = 1 - (S_M + W_M)$

$S_M = S_C \cdot C_M / C_C$

$$C_m = \frac{1-W_m}{1+\frac{S_c}{C_c}}$$

The proportions calculated for the establishment of the different mortars are illustrated below.

Table 4: summary table of formulations

mineralogical nature	hight-performance concrete (HSC) -C70/85			high-performance mortar (HSM)		
	HSC-N black limestone	HSC-X flint	HSC-G granite	HSM-SN black limestone	HSM-SX flint	HSM-SG granite
cement CEM I 52,5 [kg]	500	500	500	832	842	850
cement volume [m3]	0,161	0,161	0,161	0,268	0,271	0,274
sand [kg]	711	694	677	1179	1327	1259
sand volume [m3]	0,289	0,282	0,276	0,482	0,476	0,470
S/C ratio by volume	1,795	1,75	1,71	1,795	1,752	1,714
S/C ratio by mass	1,422	1,388	1,354	1,417	1,576	1,482
E/C ratio by mass	0,3	0,3	0,3	0,3	0,3	0,3
water [kg]	150	150	150	250	253	256
superplastifizer [kg]	4,2	5,3	3			
% cement	0,84%	1,06%	0,60%			
by 100 Kg of cement [kg]	0,84	1,06	0,6			
superplastifizer volume [l]	3,89	4,91	2,8			
density fresh [kg/m3]	2432	2406	2399			
density fresh calculated [kg/m3]	2411	2380	2360	2261	2422	2366
fc90 [Mpa]	86,86	75,41	80,83			
ft90[Mpa]	5,66	4,7	5,2			
E[Mpa]	45,79	53,43	46,3			
compacteness ϒ (sans eau)	0,85	0,85	0,85	0,75	0,75	0,74
compactness ϒ	1	1	1	1	1	1
granular class [mm]				0/4	0/4	0/4
real density [kg/m3]				2447	2790	2680
absorption coefficient [%]				0,48	1,05	0,45

The quantities are defined. We must now introduce the correction of water, in order to respect as best as possible the established formulation. Sands are not dried to 100% upon creation of mortars, the sands contain a certain degree of humidity that must be taken into account. Moreover, the absorption coefficient at 24 W_{24} calculated above ensures that a portion of the water to be introduced will be absorbed by the sand. If this phenomenon is not corrected, the total volume will be distorted and the formulation will not be respected.
The calculation for finding the right correction is the following.
Correction on the quantities of material considering the water content per 1 m^3 of mortar

Quantity of sand:

$$S = S_{initial} \cdot (1 + W_S\,\%)$$

Where

S [Kg]: amount of sand to be implemented

$S_{initial}$ [Kg] : quantity of sand theoretically calculated

W_S % [%] : water content at the time of manufacture

Quantity of water (water content) :

$$W = W_{initial} - S\ (W_S\ \% - WA_S\ \%)$$

Where

W [Kg] : amount of water to be implemented

$W_{initial}$ [Kg] : quantity of water theoretically calculated

WA_S % [%] : sand water absorption

For each type of mortar, we have created three samples of 40x40x160 mm with a total volume of 0.768 l.

Table 5: compactness volume

	B-LIMESTONE	FLINT	GRANITE
Wm [kg]	250	253	256
Wm [m3]	0,25	0,253	0,256
Cm [m3]	0,268	0,271	0,274
Sm [m3]	0,482	0,476	0,470
Wm [kg]	250	253	256
Cm [kg]	657	757	735
Sm [kg]	1179	1327	1259

Table 6: formulation for each sand

	b-limestone	flint	granite
wet mass[kg]	0,164	0,162	0,158
dry mass [kg]	0,159	0,153	0,151
water content [%]	3,41	5,31	4,18
loss coefficient	1,20	1,20	1,20
volume for cast [l]	0,768	0,768	0,768
real volume for cast [l]	0,92	0,92	0,92
cement [kg] for 1 m3	832	842	850
cement [kg] for cast	0,767	0,776	0,783
sand [kg] for 1 m3	1219	1397	1312
sand [kg] for cast	1,12	1,29	1,21
water [kg] for 1 m3	214	193	207
water [kg] for cast	0,197	0,178	0,191

Three prismatic specimens with dimensions of 40x40x160 mm are prepared for each mixture following the procedure described in EN 196-1. The mortar is prepared by mechanical mixing and is compacted in a mould using a standard jolting apparatus. The specimens in the mould are stored in a moist atmosphere for 24 h and then demoulded specimens are stored under water for 28 days and then they are cut and reduced to powder for thermal analyzes.

PREPARATION OF MORTAR [EN 196-1]

Laboratory and equipment

The laboratory where preparation of specimens takes place shall be maintained at a temperature of 20°C and a relative humidity of not less than 50%. The moist air room for storage of the specimens in the mould shall be continuously maintained at a temperature of 20°C and a relative humidity of not less than 90%.

Mixer

The mixer shall consist essentially of:

- A strainless steel bowl with a capacity of about 5l
- A strainless steel blade of the general shape, size and tolerances shown in figure

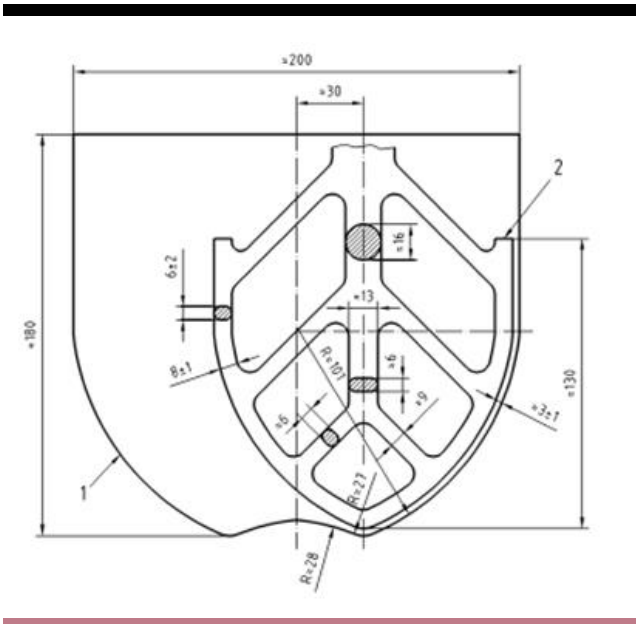

Figure 10: bowl and blade

Mould

The mould shall consist of three horizontal compartments so that three prismatic specimens 40x40 mm in cross section and 160mm in length can be prepared simultaneously.
A typical design is shown in figure:

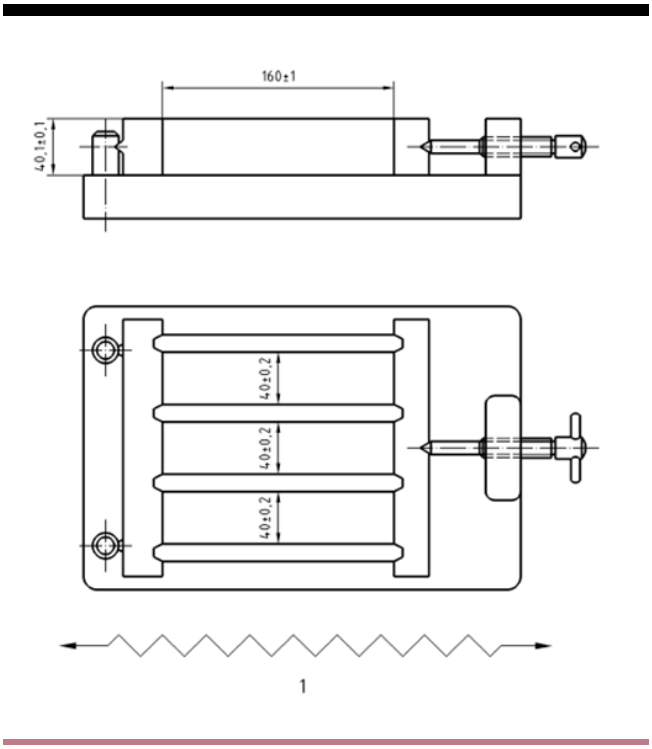

Figure 11: typical mould

Jolting apparatus

The jolting apparatus consist essentially of a rectangular table rigidly connected by two light arms to a pivot at 800mm from the center of the table as shown in figure:

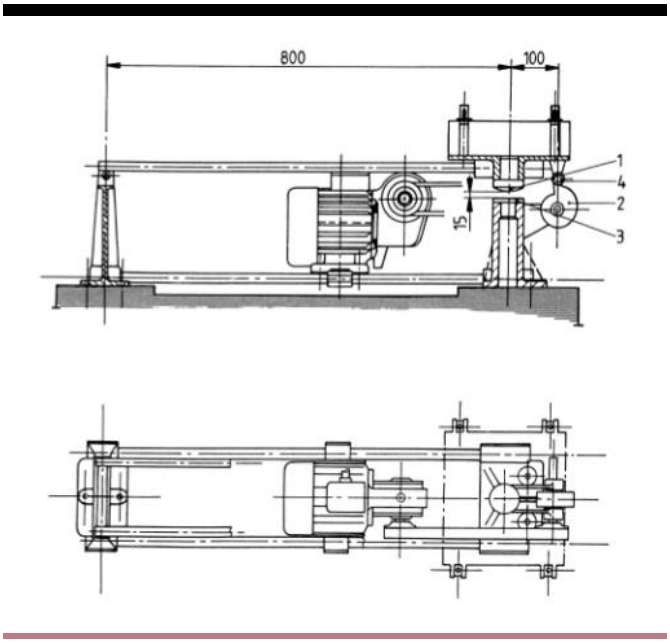

Figure 12: typical jolting apparatus

MODUS OPERANDI: MORTAR PREPARATION

The cement, sand and water and apparatus shall be at the laboratory temperature. Mix each batch of mortar mechanically using the mixer. With the mixer in the operating position:

-pour the water into the bowl and add the cement

-then start the mixer immediately at the low speed and, after 30s add the sand steadily during the next 30s. Switch the mixer to the high speed and continue the mixing for an additional 30s

-stop the mixer for 1min 30s. During the first 15s, remove by means of a rubber scraper all the mortar adhering to the wall and bottom part of the bowl and place in the middle of the bowl.

-Continue the mixing at the high speed for 60s.

Figure 13: mixer

Mould the specimens immediately after the preparation of the mortar. Then compact the fist mortar layer using 60 jolts. Introduce the second layer of mortar, level with the smaller spreader and compact the layer with a further 60 jolts.

Demoulding after 24 h with due precautions. Keep the demoulded specimens covered by a damp cloth until tested. Suitably mark specimens selected for curing in water for identification later, e.g. by water-resistant ink.

Figure 14: jolting apparatus

After leaving specimens in a room at 20 ° C with humidity of not less than 90%; they are cut with the saw and ground to powder for thermal analysis.

Figure 15: mould after 24h

Figure 16: specimens covered by a damp cloth

I.2. Thermal analysis

Thermal analysis is a branch of materials science where the properties of materials are studied as they change with temperature. Several methods are commonly used, these are distinguished from one another by the property which is measured:

- DILATOMETRY (DIL) = volume
- THERMOGRAVIMETRIC ANALYSIS (TGA) = mass
- DIFFERENTIAL SCANNING CALORIMETRY (DSC) = heat difference

I.2.1. Dilatometry

To better understand the behavior of the aggregates and the cement at high temperatures we proceed with dilatometer test method.
Dilatometry is a thermomechanical technique for the measurement of expansion or shrinkage of solids, powders, pastes and liquids under a controlled temperature/time

program. A precise understanding of this behavior can provide insight into firing processes, the influence of additives and raw materials, densification and sintering properties, reaction kinetics, phase transitions, and thermal shock. In addition, it can be used for glaze development and to match CTEs (glaze-ceramic, metal-ceramic in the automotive industry).
Dilatometry can be applied not only to solid samples, but also to powders, pastes, and even liquids. It can also be used to carry out rate-controlled sintering studies on reactive powders in fields such as advanced ceramics or powder metallurgy.

In the bibliography we can find dilatometer method to measure as-received aggregate coefficient of thermal expansion (CoTe) or to determining ASR characteristics.
The coefficient of thermal expansion (CoTE) is a fundamental engineering material property that quantifies the change in unit length per degree of temperature change. The thermal expansion/contraction behavior due to daily and seasonal temperature changes plays an important role on the degree of opening/closing of transverse cracks in concrete structures and pavements as well as development of related crack patterns and is perhaps a contributor to pavement distresses such as blowups, faulting, corner breaks, and spalling in continuously reinforced concrete pavements.
A dilatometer can accommodate materials of different size, shape, and density.
Test methods developed in the past to measure aggregate CoTE included one developed by Willis and DeReus(1939) witch was based on the measurement of vertical movement of the tested specimen by an optical lever (by reading the image reflected by the mirror of the optical lever) over a considerable temperature range (3°C to 60°C). The specimens used in this test method were cores of 25.4 mm diameter and 50.8 mm long drilled from the aggregate specimens to be tested and placed in a controlled temperature oil bath.
The use of a strain gauge constitutes another method to determine aggregate CoTE. This method of measurement focused on the linear aggregate expansion over a set temperature range. The method developed by Mitchell (1953) uses 25.4 x 76.2 mm specimens coated with wax and held in a fulcrum-type extensometer frame.
Electromagnetic strain gages with electronic indicators are used to do the measurement while the specimen is immersed in a circulating ethylene glycol solution at the desired temperature range. Therefore, the strain gauge method needs special sample preparation such as preparing smooth surfaces of aggregate particles within a specific size range which limits testing materials consisting of small particle sizes (fine aggregate). Verbeck and Hass (1951) developed a dilatometer method for determining the cubical CoTE of sand and coarse aggregate. The method was specifically adopted to measure CoTE of sands and also provided a means of obtaining and testing a representative sample of a heterogeneous coarse aggregate or of the various mineralogical portions comprising the coarse aggregate. The apparatus consisted of a 1000 cc dilatometer flask to which was attached a laboratory-constructed capillary bulb arrangement containing electrical contacts spaced over a calibrated volume. The apparatus was calibrated to determine the coefficient of volumetric thermal expansion of the flask. The aggregate sample was immersed in water for a few days in order to ensure substantial filling of surface accessible voids by absorption of water by aggregate.
In operation, the flask was filled with aggregate and water and allowed to equilibrate at one of the controlling electric contacts. The equilibrium temperature is noted, and the procedure is then repeated at the other electrical contact. After calibration, the only measurements

required are the weight of the water placed in the flask and the temperature needed to produce an expansion equivalent to the volume between the electrical contacts.
the objective of the subject study was to develop a dilatometer-based test method to measure the bulk CoTE of aggregates.
The dilatometer methodology most present in bibliography can accommodate a variety of materials (e.g., loose coarse aggregate, fine aggregate, material of single mass with any size, core samples, etc.) and as a consequence is a versatile CoTE measurement technique. Although substantial differences exist in the sample preparation and the design and method of data acquisition between it and the one developed earlier by Verbeck and Hass (1951), the basic theory of measurement remains almost the same.

Dilatometer Device

The dilatometer test device consists of a stainless steel container, a brass lid, a glass float (to which a LVDT is attached), a thermocouple, and a data acquisition system.

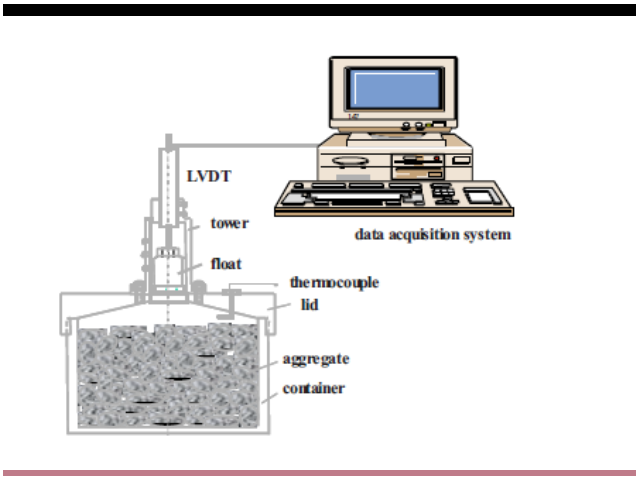

Figure 17: schematic description of a dilatometer

Aggregate is placed into the chamber of a metallic container having an enlarged opening. The aggregate is placed in a water bath, and a tightly sealable lid is placed onto the container. The lid carries a linear variable differential transducer (LVDT). A thermocouple for sensing temperature is also retained within the lid so that a sensor on the thermocouple contacts the water bath when the lid is secured onto the container. The LVDT is operationally interconnected with a storage or recording device. In a preferred constructions the lid retains a tower member having a float that is freely moveably mounted upon a guide rod. Movement of the float is indicative of a volumetric change in the aggregate and water. In operation, the dilatometer device is used to determine the information relating to the amount of expansion or contraction of the aggregate in response to thermal changes.
Sample preparation involves

- 24 h water soaking of thoroughly washed representative aggregate samples
- determination of aggregate saturated surface dry (SSD) and submerged weight
- The aggregate, after being placed in the dilatometer with water is subjected to deairing (done in two parts while vacuuming under vibration first at room

temperature (≈45 min) followed by an additional vacuuming at 80°C (≈45–60 min)to remove the air bubbles effectively from the water, material interfaces, and interior pores of the aggregate particles. However, high absorptive aggregates need some special attention (e.g., boiling) to ensure full saturation of aggregates pores.

- After deairing, the water level is adjusted to a certain graduation mark in the tower to make the initial water level same for all the tests.

The dilatometer with the materials to be tested and water inside is placed in a water bath and subjected to a temperature change from 10 to 50°C.

The thermal expansion of both tested material and water causes the water level to rise whereas the thermal expansion of the container causes the water level to go down in the tower. The resultant water level rise of the combined thermal expansion of the tested material, water and dilatometer container is recorded by a LVDT through the movement of a float, which is placed in the water in the tower.

The temperature and float displacement are recorded by a data acquisition system LVDT. The LVDT is calibrated to record 1/100 mm of displacement.

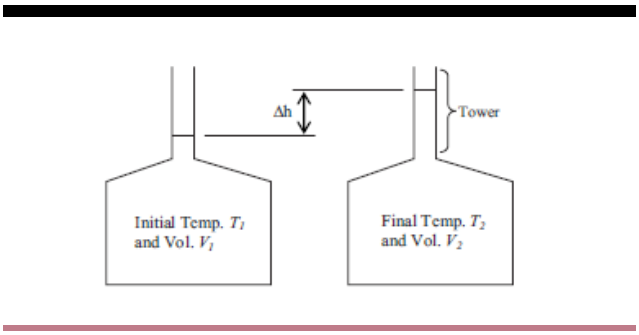

Figure 18: schematic representation of the initial and final states of the dilatometer test parameters

The initial volume V_1 represents volume of water V_w plus volume of the tested materials V_a (volume of the aggregate) at initial testing temperature T_1 and final volume V_2 represents the same ($V_w + V_a$) at the final temperature T_2. The data acquisition system records the float movement as the water level changes in the tower ($\Delta h=h2-h1$) with change of temperature ($\Delta T=T_2-T_1$). It takes approximately 5 h to complete a test run with

- 1 h for cooling from room temperature to 10°C
- 1.5-h stabilization at 10°C
- 1 h for heating from 10 to 50°C
- 1.5-h stabilization at 50°C.

The apparent volume change that the LVDT detects can be expressed mathematically as

$$\Delta V_1 = A\,\Delta h = \Delta V_a + \Delta V_w - \Delta V_f$$

Where

- ΔV_1 observed total volumetric increase due to temperature change ΔT
- A inner section aerea of tower
- Δh rise of the water surface inside the tower
- ΔV_w volumetric increase of water due to temperature Δt
- ΔV_f volumetric increase of internal volume of the flask due to ΔT
- ΔV_a volumetric increase of tested material due to ΔT

$$V_f = V_a + V_w = V$$

$$\Delta V_a = V_a \gamma_a \Delta T$$

$$\Delta V_f = V \gamma_f \Delta T$$

$$\Delta V_w = V_w \gamma_w \Delta T = (V - Va) \gamma_w \Delta T$$

Where

- V total internal volume of the flask
- V_w volume of water in tha flask
- V_a volume of tested material in the flask
- γ_a coefficient of volumetric thermal expansion of water
- γ_f coefficient of volumetric thermal expansion of the flask
- ΔT temperature increase from T_1 to T_2

The final equation to calculate the volumetric CoTe (γ_a) of the tested material can be derived as

$$\gamma_a = 1/V_a (A \Delta h/ \Delta T - V_w \gamma_w + V_f \gamma_f)$$

where $V_w = V-V_a = V_f - V_a$

Among the parameters on the right-hand side of the Equation the cross-sectional area of the tower A is a fixed value for the dilatometer. The volumetric thermal coefficient of the container γ_f is basically a fixed composite parameter that addresses the internal volume of the flask, which is represented by combined internal volume of the container, lid, and tower of the dilatometer. Other parameters, Δh, T, V, V_a, and Υ_w, are variable and they are either directly measured (Δh,T,V,Va) or estimated (Υ_w) based on the collected data. It has been shown that the linear CoTE of an isotopic material is one third of the volumetric CoTE which provides sufficient simplification to assure the practicality of the test procedure.
The dilatometer test method has been developed and validated against CoTe measures for steel, selected pure minerals, and some common aggregates using the last equation.

The dilatometer used in this experience is DIL 402 PC NETZSCH

Figure 19: DIL 402 PC NETZSCH

METHOD AND PRINCIPLE OF DILATOMETRY

Pushrod dilatometry is a method for determining dimensional changes versus temperature or time while the sample undergoes a controlled temperature program. The degree of expansion divided by the change in temperature is called the material's coefficient of expansion (α) and generally varies with temperature.

$$\alpha = \frac{1}{L_o \frac{\Delta L}{\Delta T}}$$

where
α = coefficient of expansion
L_0 = initial sample length
ΔT = change in temperature
Δl = change in length

To perform a dilatometric analysis, a sample is inserted into a special holder within a movable furnace. A pushrod is positioned directly against the sample and transmits the length change to a linear variable displacement transducer (LVDT). As the sample length changes during the temperature program, the LVDT core is moved, and an output signal proportional to the displacement is recorded. The temperature program is controlled using a thermocouple located either next to the heating element of the furnace or next to the sample. Since the sample holder and the front part of the pushrod are being exposed to the same temperature program as the sample, they are also expanding. The resulting dilatometer signal is therefore the sum of the length changes of sample, sample holder, and pushrod. It is thus necessary to correct the raw dilatometer data in order to obtain a true view of sample behavior. There are two correction methods: the application of tabulated expansion data, or, often more precise, of a correction curve to eliminate systematic error.

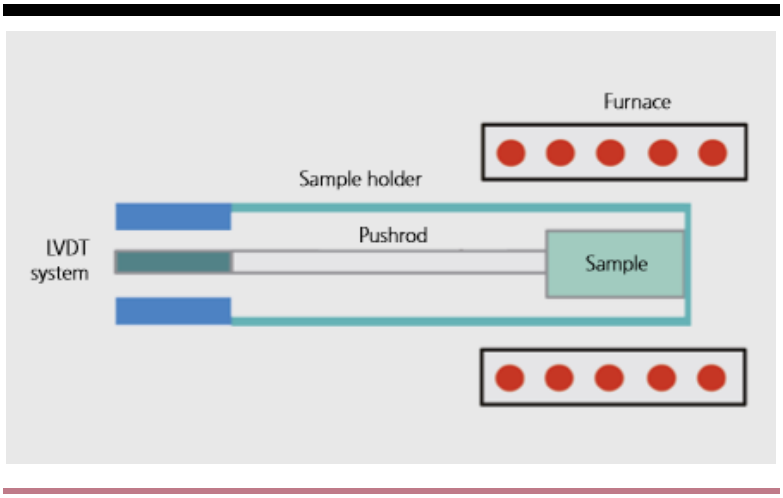

Figure 20: schematic of a pushrod dilatometer

The DIL 402 PC is specially tailored to the needs of the sands, aggregates and glass industry. High resolution and stability, a wide measurement range, and a robust and compact design are only some of the many advantages of this cost-effective instrument. The optimized design of the measurement system with inductive transducer compensates for temperature fluctuations and yields highly reproducible data. A chiller is not required.
The DIL 402 PC are based on nearly all national and international standards. The instrument has a horizontal design with an easy-to-operate furnace. A large recess in the tube-type sample carrier facilitates the placement of samples even when their geometries are less than ideal. A thermocouple in direct proximity to the sample ensures reproducible temperature measurement.

PRINCIPLE OF OPERATION

The sample is placed in the homogenous temperature zone of the furnace. The furnace is heated according to a preselected temperature program. The furnace temperature is controlled by the control thermocouple. The sample is submitted to a temperature-dependent change in length. The sample temperature is measured by the sample thermocouple. Sample carrier and pushrod are also submitted to a change in length. Thus there is measured and registered the sum of change in length of the sample, the sample carrier and the pushrod. The pushrod transmits this change in length mechanically to the displacement transducer (LVDT) and causes a displacement of the core of the displacement transducer (LVDT). The resulting change in voltage is transformed by a carrier frequency measuring amplifier to a d.c.voltage which is proportional to the displacement. The signal is registered by the computer.

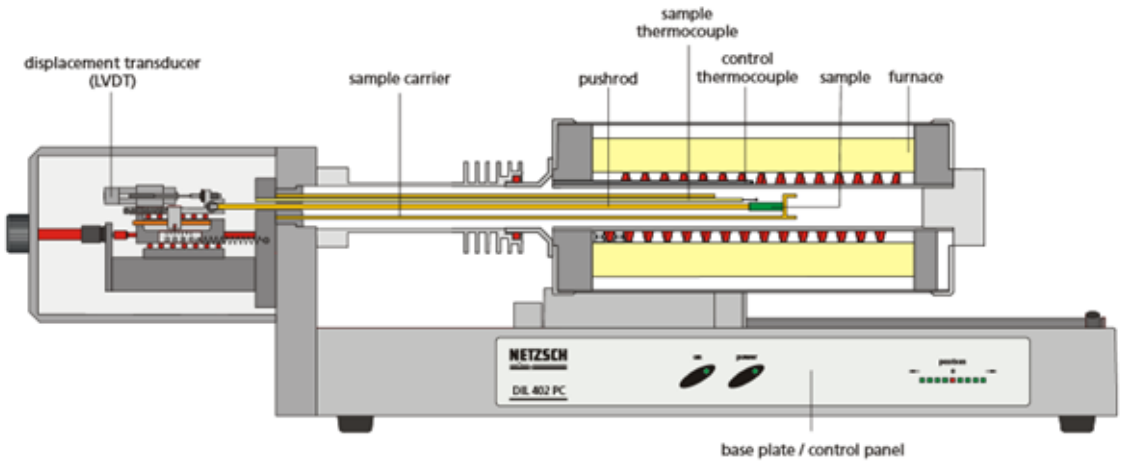

Figure 21: schematic diagram of DIL 402 PC

The interchangeable furnaces with temperature ranges up to 1200°C and 1600°C allow for the analysis of expansion in solids, green bodies, powders and pastes, for production and quality assurance purposes across a variety of applications. The forced-air cooling system of the
1600°C furnace makes it possible to cool faster from maximum sample temperature down to room temperature.
With automatic softening point detection, even samples which exhibit a tendency to melt can be run without any special care. As soon as a defined threshold value is reached, the software either stops the measurement or jumps directly to the next segment of the temperature program. Exchangeable sample holder systems made of alumina and fused silica are available. The maximum sample dimensions are 50 mm in length with a diameter of up to 12 mm (optionally 19 mm).

OPERATION

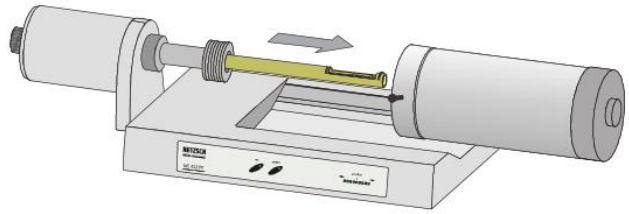

- Slide the furnace to the right limit stop

- if necessary, place sample supports in the sample holder.

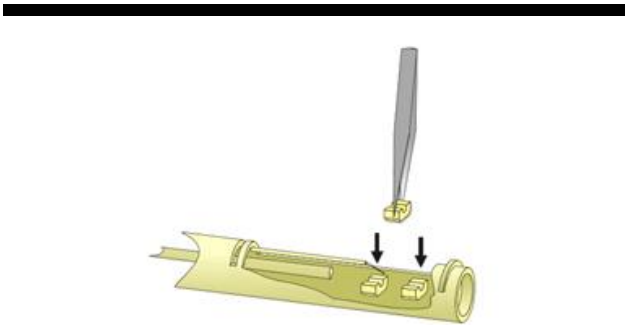

- Place the standard sample on the sample supports

- Using the adjusting screw, slide the pushrod towards the sample.

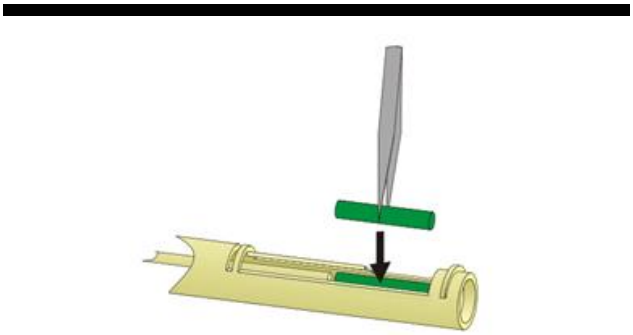

- Position the thermocouple close to the sample. The thermocouple must not come into contact with the sample.

- Slide the furnace carefully to the left to the limit stop.

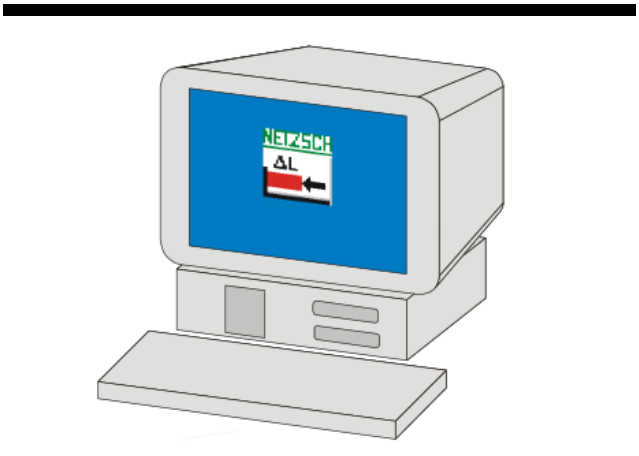

- The sample holder must not come into contact with the protective tube.

- Start the measurement software

I.2.2.ATG-DSC analysis

- THERMOGRAVIMETRIC ANALYSIS (TGA) = mass
- DIFFERENTIAL SCANNING CALORIMETRY (DSC) = heat difference

Thermogravimetric analysis (TGA) allows to measure the change in mass of the specimen as a function of temperature, while the differential scanning calorimetry (DSC) allows to identify which type of transformation/physico-chemical reaction takes place in the specimen during heating. Heat exchanges are measured between the test sample and an inert reference in the temperature range studied. In this case the reference sample is an empty alumina crucible.
Thermogravimetry (TGA) and Differential Scanning Calorimetry (DSC) refer to the same sample in one instrument: STA 449 F1 Jupiter.

Figure 22: insertion of the specimen in the measuring instrument STA 449 F1 Jupiter

Are subjected to thermal analyzes:

- Flint sand mortar [HSM-SX]
- Black limestone sand mortar [HSM-SN]
- Granite sand mortar [HSM-SG]
- Ordinary cement paste [NP]
- High-performance cement paste [HSP]
- Flint sand [SX]
- Black limestone sand [SN]
- Granite (pink part) sand [SGp]
- Granite(black part) sand [SGb]

Granite sand is divided into two parts: the black part composed of micas and the pink part, this is done to better understand the influence of the micas and to analyze its behavior at high temperatures.

Figure 23: granite sand, pink part

Figure 24: granite sand, black part

The specimens are dried in an oven for 48h and then pulverized and kept in small sealed bags, to not be contaminated with the environment humidity.

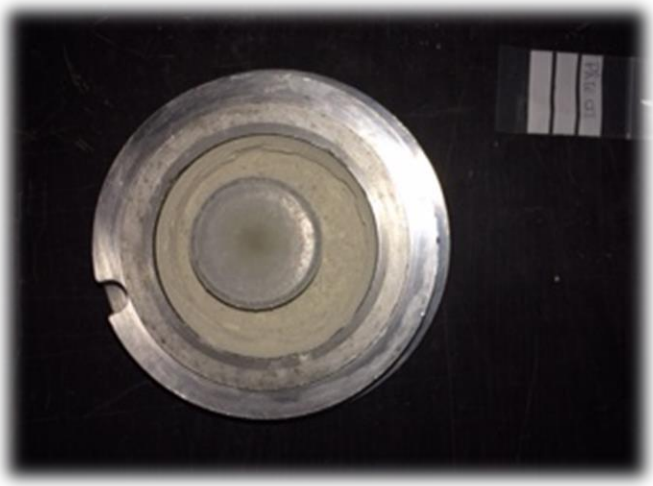

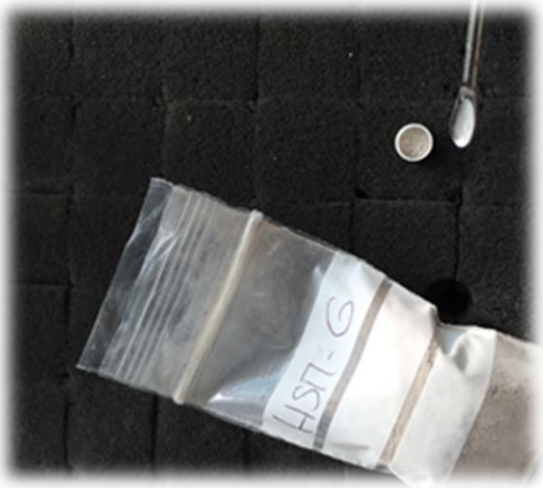

Figure 25: instrument used to pulverize

Figure 26: sealed bag and crucible

A small amount of material, about 50 g is inserted into the crucible and subjected to thermal analysis. The balance of the instrument is calibrated, then the weight of the specimen is measured, taking into account the correction made before the start of the experiment.

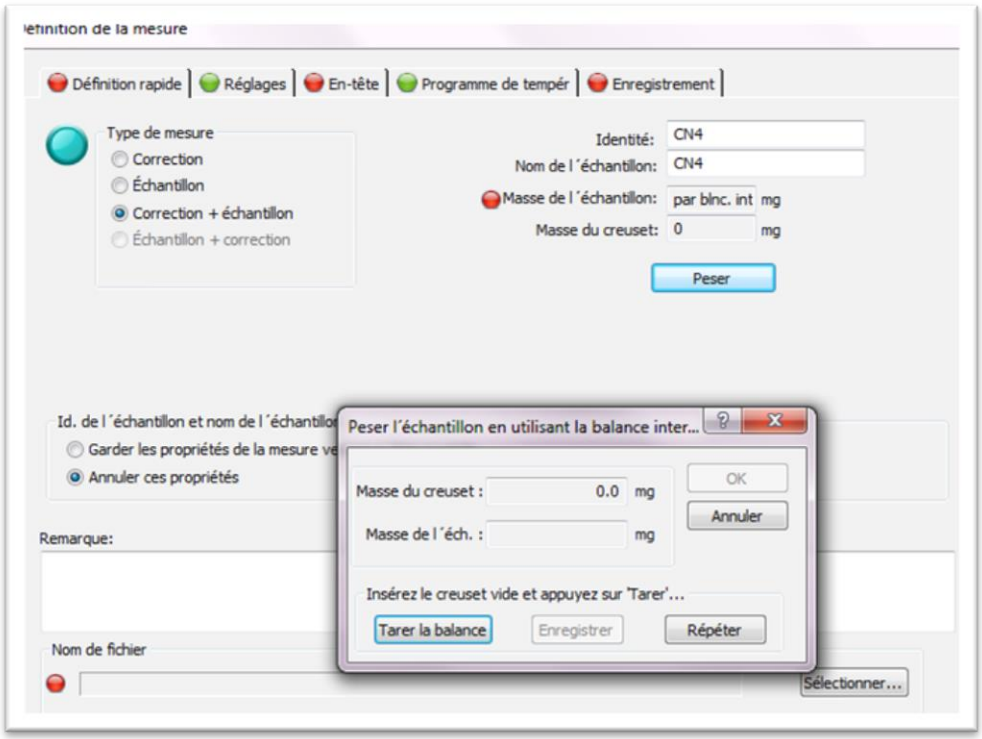

Figure 27: definition of measures

The specimens are subjected to elevated temperatures ranging from 20 ° C to 1000 ° C. The heating rat is 10 K/min. For each specimens are conducted three tests.

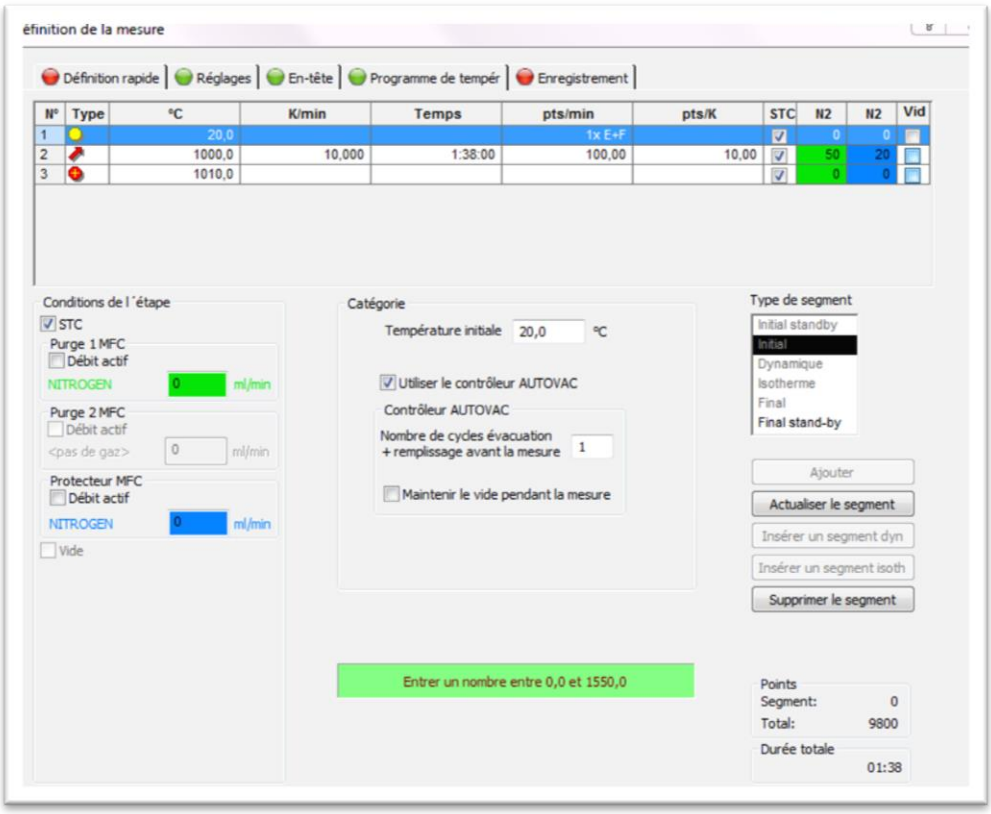

Figure 28: temperature program

CHAPTER II: Results and discussion

II.1. Dilatometry

Dilatometry is a thermomechanical technique for the measurement of expansion or shrinkage of solids, powders, pastes and liquids under a controlled temperature/time program.
Specimens with parallelepiped shape (10x10x45mm) are used in order to respect the size of the instrument used. Three different mortars are prepared by using ordinary Portland cement, granite sand, flint sand and black limestone sand.

Table 7: normal mortar formulation for $1m^3$

mineralogical nature	normal mortar (NM)		
	NM-SN black limestone	NM-SX flint	NM-SG granite
cement CEM I 52,5 [kg]	622	615	637
cement volume [m3]	0,201	0,198	0,205
sand [kg]	1128	1303	1201
sand volume [m3]	0,461	0,467	0,448
S/C ratio by volume	2,30	2,35	2,180
S/C ratio by mass	1,81	2,12	1,89
W/C ratio by mass	0,54	0,54	0,54
water [kg]	339	335	347
density fresh [kg/m3]	2101	2210	2164
density fresh calculated [kg/m3]	2088	2252	2184

The specimens are subjected to a elevated temperatures ranging from 20 ° C to 1000 ° C and cooling cycle (from 1000 °C to 20°C). The heating rat was 10 K/min.
For each aggregate are conducted three tests; the graphs of expansion are exposed below for each type of aggregate.
Furthermore, the specimens were observed before and after the test, to see how it changes the morphology and the color of the material.

a. Flint mortar

Figure 29 : flint mortar before dilatometry

Figure 30: flint mortar after dilatometry

After the cycle of heating / cooling the sample of flint does not show important deterioration.

The flint mortar is not subject to significant cracking, the small cracks that can be noticed are organized reticular form. The incompatibility of deformation generates small cracks at the interface cement paste and aggregate, these cracks propagate and degrade the cement matrix as low as 300 ° C, should be noted that these cracks do not cross the aggregates. Micro-cracks arise at high temperatures in the aggregate, independent of external cracks between cement paste and aggregate. The flint mortar at the end of the process of heating and cooling has changed color, becoming much more clear, tending towards white, this change is due to the presence of iron in flint sand and to the lime in cement paste.

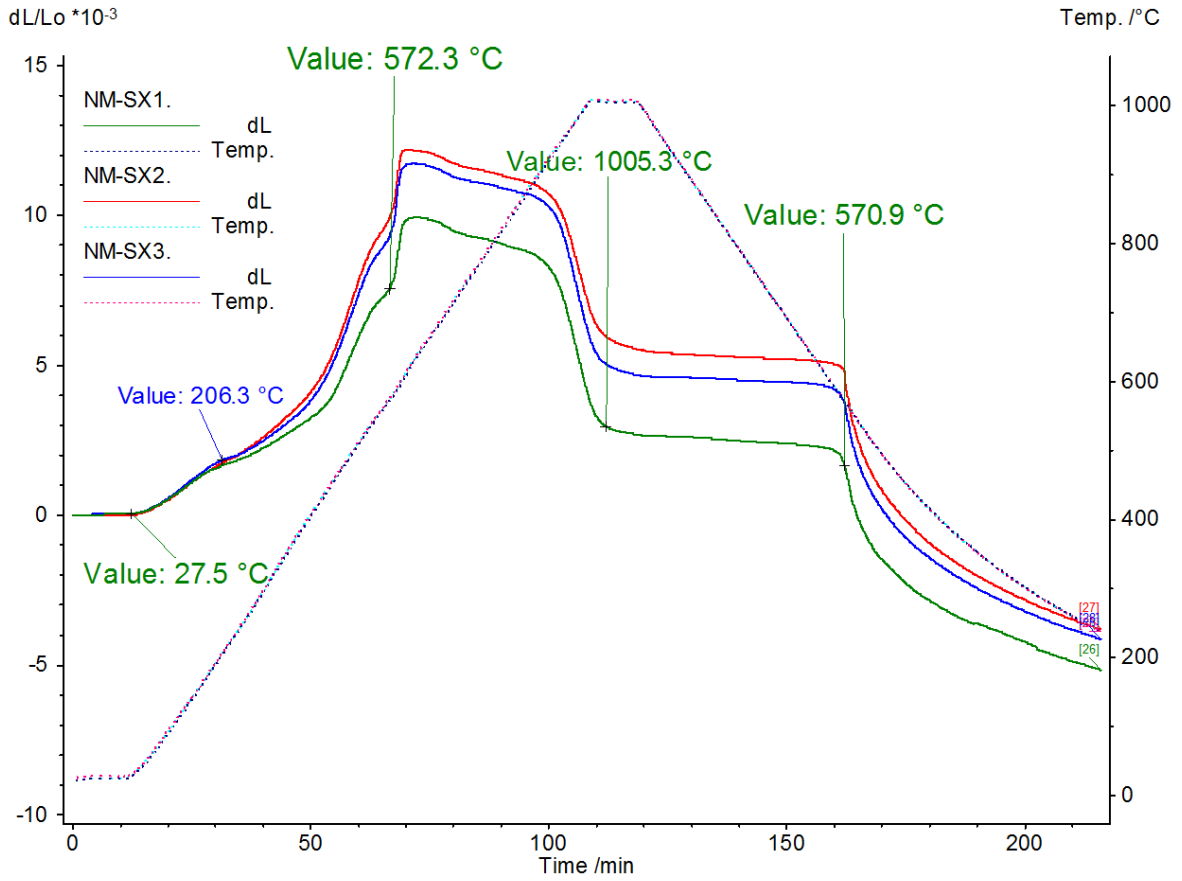

Figure 31 : Expansion curve : flint mortar (NM-SX)

From the observation of the expansion curve it easy to notice how the dilation begins around 27 ° C until reaching a maximum value around 600 °C.
This sharp increase is due to the allotropic transformation of quartz α that becomes quartz β around 573°C.
At 200 ° C there is a variation of the gradient, this may be due to cement, in fact, the gel of the cement undergoes a degradation starting at 180 ° C with loss of water chemically bound.
After reaching 1000 ° C cooling begins, the material starts to retreat up to the until transformation of quartz β into α quartz around 570 ° C, you can see from the chart a sharp slope.

b. Granite mortar

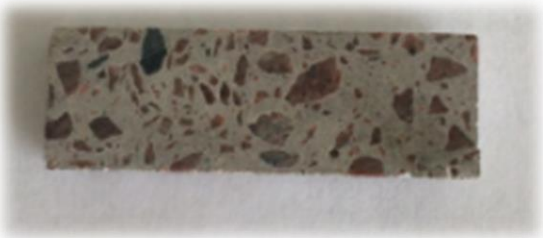

Figure 32: granite mortar before dilatometry

Figure 33: granite mortar after dilatometry

From bibliography it is known that granite sand begins to crack as low as 300°C. The cracks develop in the interface between cement past and aggregates. At 450 ° C the cracks become very evident; the cracks do not traverse the aggregate.
The figure shows how the granite mortar specimen has changed color after the heating cycle, the color has become more clear, tends to pink/white. This color change is also reflected in the other two mortars. The change is due to the large amount of water in granite sand and to Cao present in cement paste that hydrates on contact with moisture environment.
The fissures are evident, despite what the material has a low resistance, only with effort it can break it with the hands.

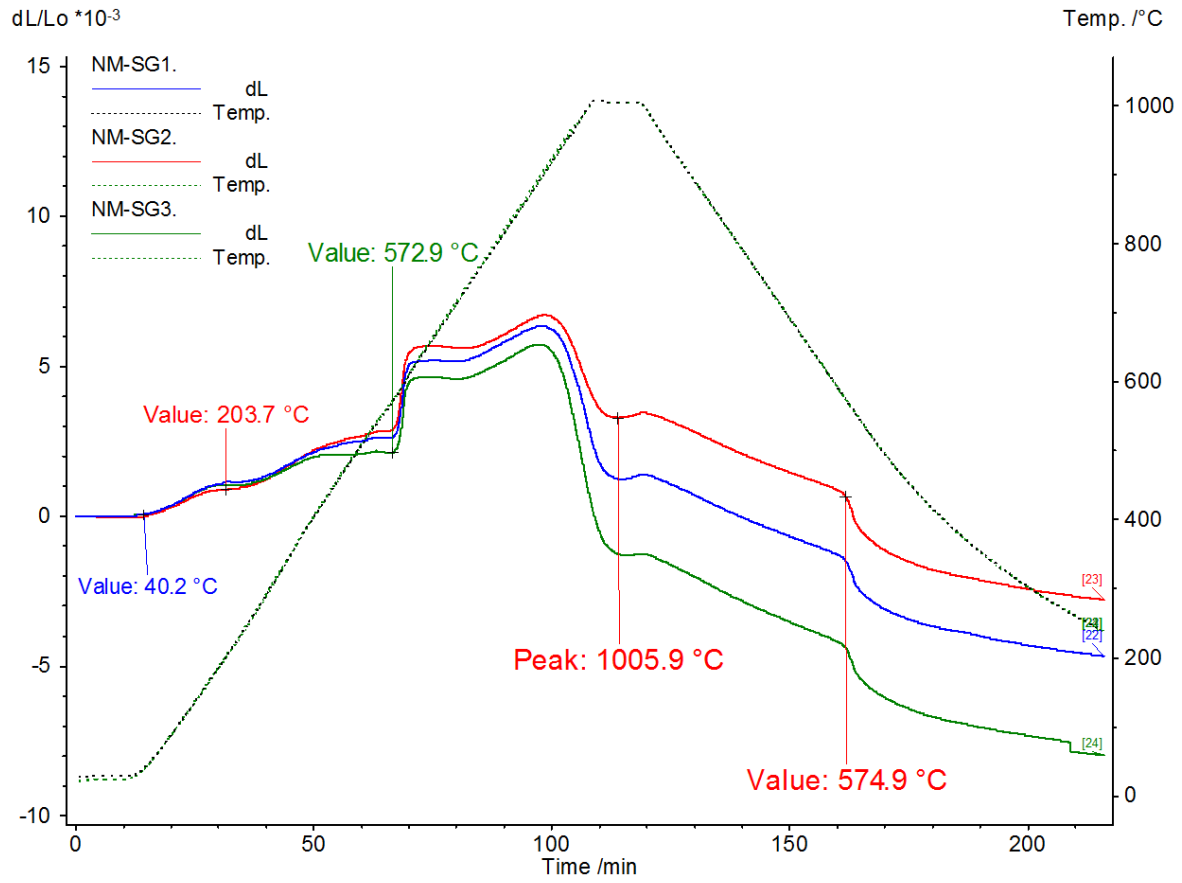

Figure 34 : Expansion curve : granite mortar (NM-SG)

The first part of the graph is very similar to that analyzed for flint, the same behavior is associated with the presence of cement paste and the amount of quartz. The expansion starts around 40 ° C, with variation of slope always around 200 ° C, due to decomposition of hydrated calcium sulphate $CaSO_4\,2H_2O$ and due to chemically bound water that comes out. Around 573 ° C takes place the transformation of quartz from α to β with a very fast expansion.
The expansion of the granite reaches the maximum level around 913 ° C.

An abrupt loss of slope is found at around 1000 ° C this could be due to the dehydration of water which is located between the filaments of the micas. Always towards 580 ° C reappears transformation of quartz β-α. This transformation shows how the process is reversible.

c. Black limestone

Figure 35:black limestone before dilatometry

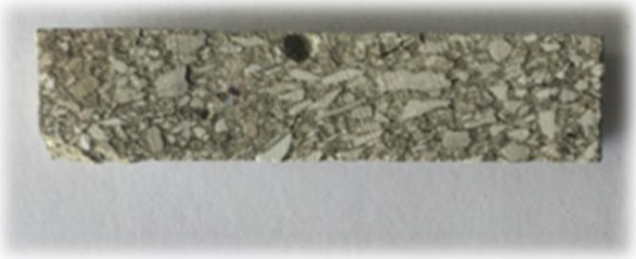

Figure 36: black limestone after dilatometry

The black limestone sand presents a chemical instability due to the calcite decarbonation that begins from 600 ° C. At 300 ° C cracks can not be seen with the naked eye, only after passing 600 ° C can be observed micro-slits. We note the presence of two types of slits: tangential cracks between cement paste and aggregates and radial cracks connecting aggregates. After passing 750 ° C a strong degradation of the sample takes place, there is a detachment between the cement paste and the aggregates; certain aggregates are cracked and others are crushed.

At the end of the cooling and after being in contact with the humidity of the ambient air we notice a white powder that wraps around the the specimen. This color variation is due to the reaction of Portlandite $Ca(OH)_2$ that becomes CaO. After a few days exposure to ambient air lime resulting from decarbonation hydrates significantly increasing volume of the specimen, the mortar deteriorates to the point of being brittle to the touch. After a long exposure to ambient air the specimens is pulverized.

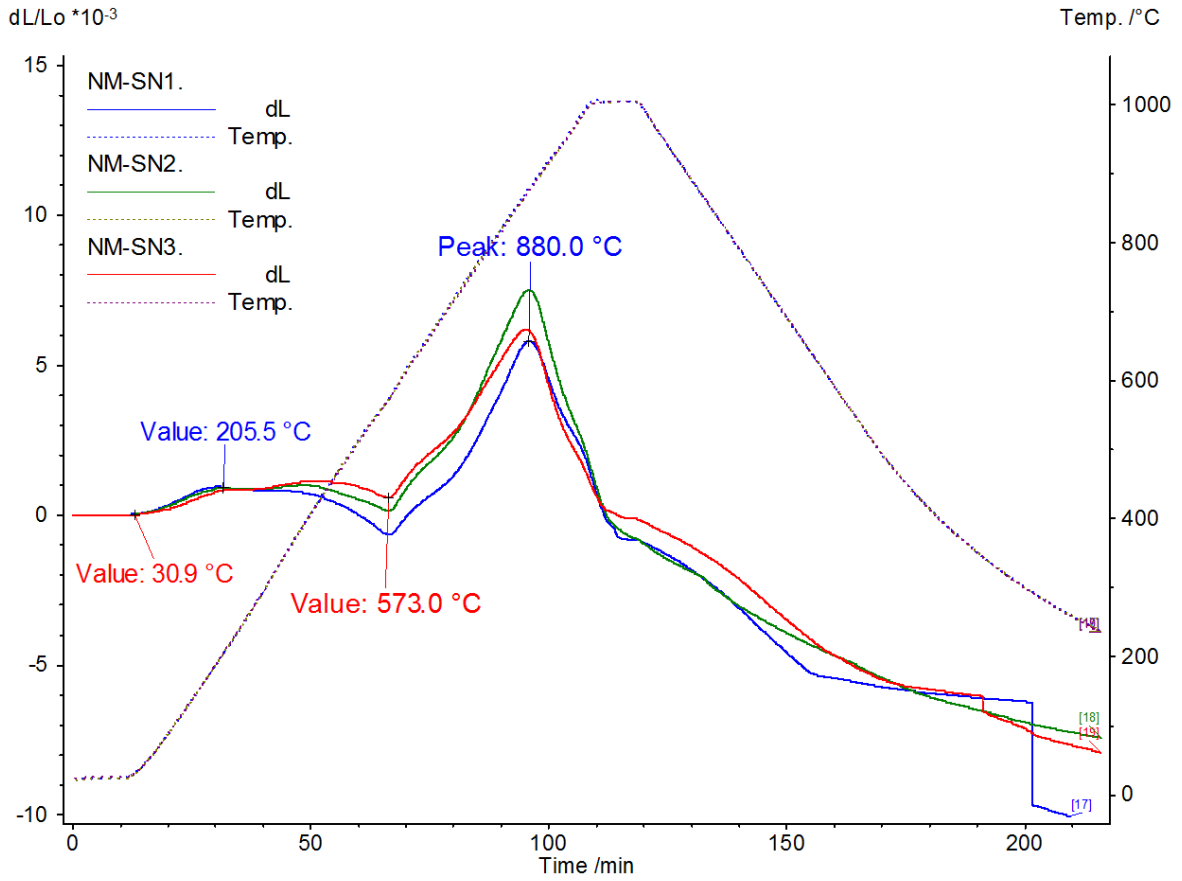

Figure 37 : Expansion curve : black limestone mortar (NM-SN)

The expansion of the black limestone begins at 24°C, the curve is maintained even up to the value of 200 ° C, where there is a loss due to dehydration of the water present in the concrete. To 573 ° C, the cement paste tends to contract much, finding little opposition by black limestone sand that expands little, this produces a lowering of the expansion curve. After the transformation of the quartz present in the cement paste there is a sharp expansion until reaching the peak at 880 °C, where take place the decomposition of calcite $CaCO_3$ in CaO.

Analyzing the expansion of three different sands there is a difference between the silica sands and limestone sand. The flint mortar and granite mortar have a very similar behavior, both having the presence of silica SiO_2. Flint sand expands more than the granite sand, this phenomenon is due to the different quantities of quartz. The gait of the expansion curve of the black limestone mortar is very different from the curves of the other two mortars, the black limestone mortar expansion curve is very steep up to reach the peak to then have a abrupt descent.

II.2. Thermogravimetric Analysis (TGA) and Differential Scanning Calorimetry (DSC)

Simultaneous Thermal Analysis (STA) generally refers to the simultaneous application of Thermogravimetry (TGA) and Differential Scanning Calorimetry (DSC) to the same sample in one instrument.
Thermogravimetry (TGA) measure change of mass and Differential Scanning Calorimetry (DSC) measure heat difference of a sample in function of temperature.
They were subjected to thermal analysis aggregates (granite, micas, flint, black limestone), mortars with different aggregates and both ordinary and high-performance concrete.
All samples were pulverized before the thermal analysis.
Below we analyze the different graphics in relation to the different aggregates and mortars.

a) Ordinary and high-performance Cement paste

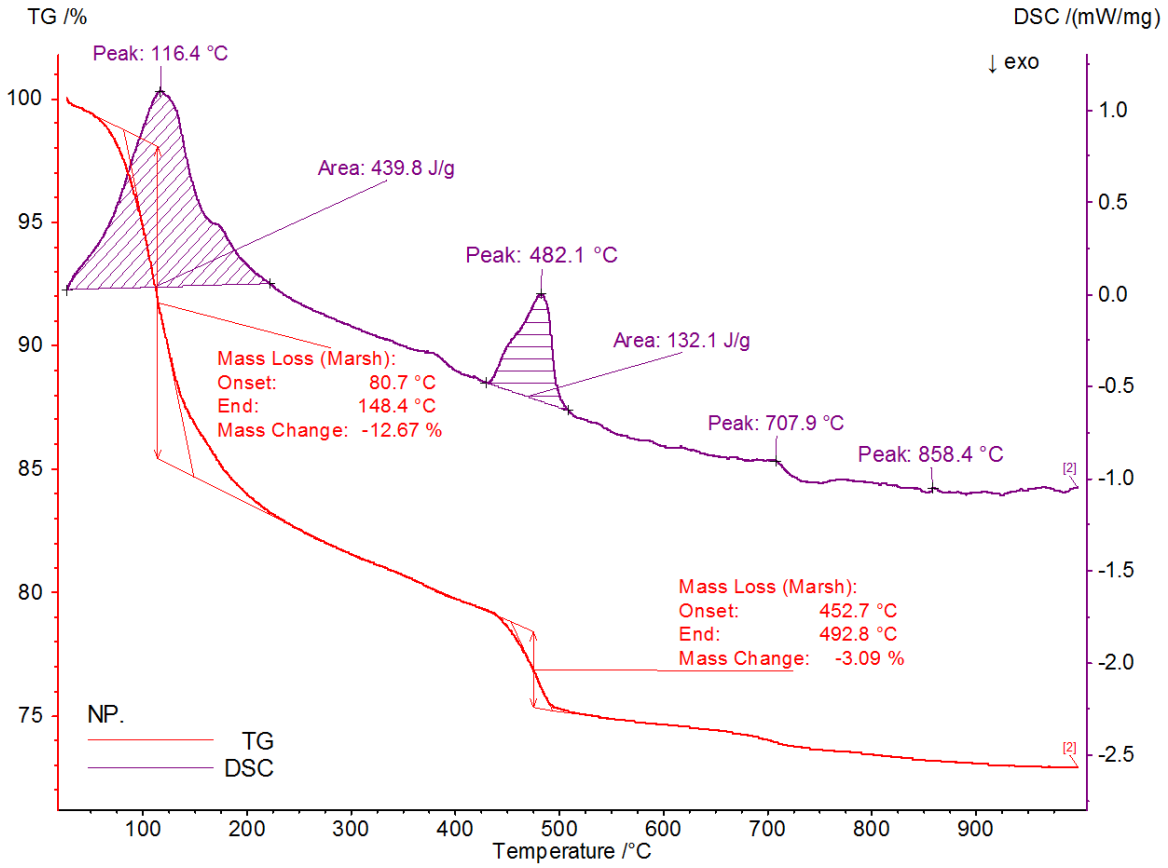

Figure 38: ATG/DSC ordinary cement paste

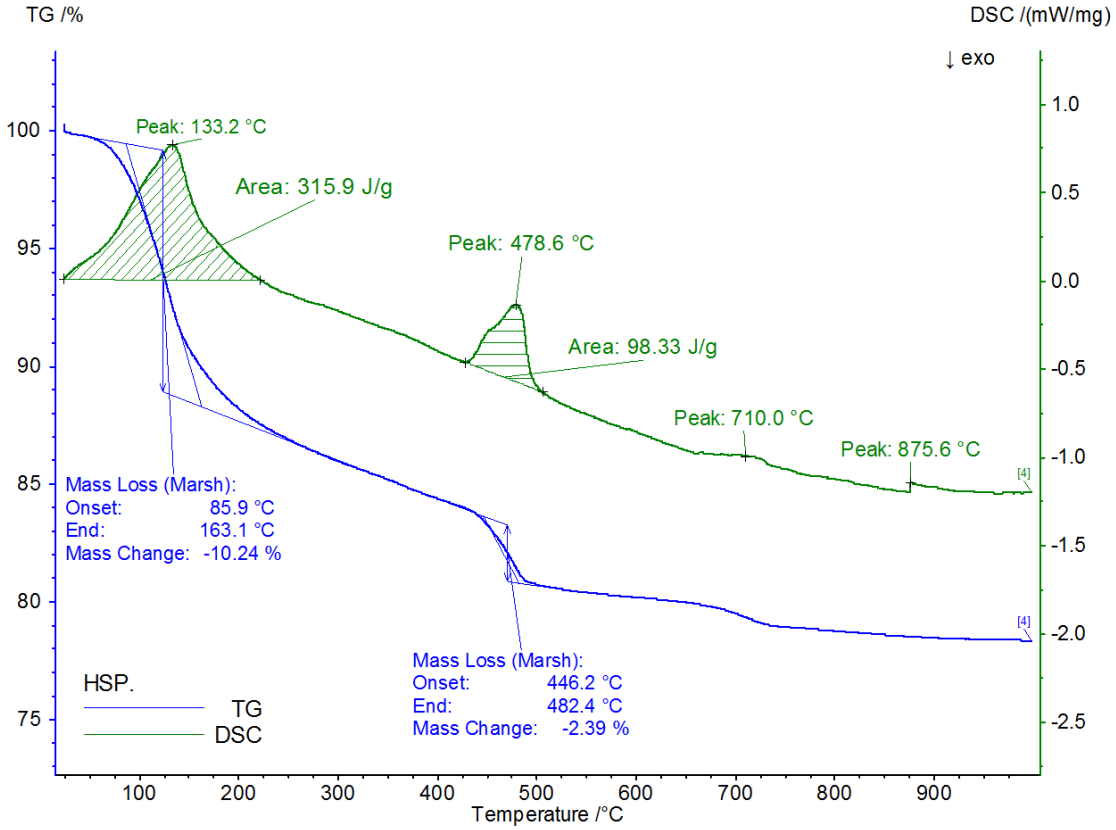

Figure 39: TGA/DSC high-performance cement paste

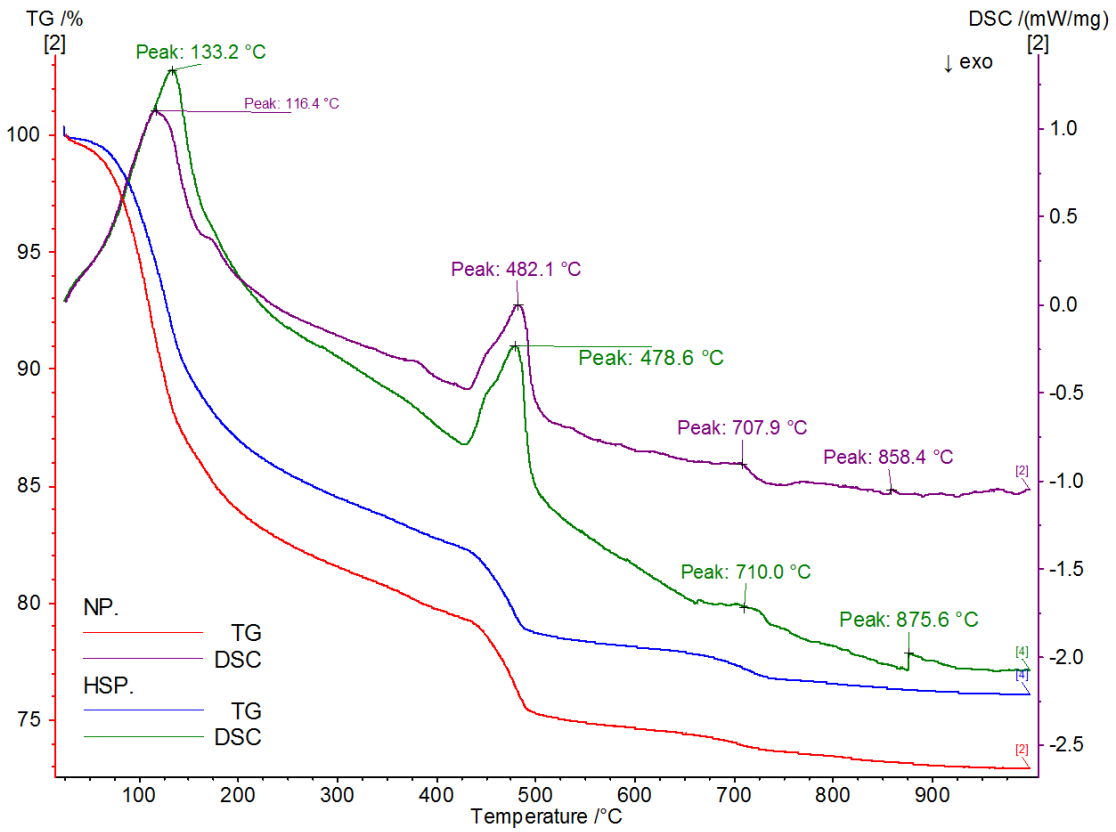

Figure 40: TGA/DSC ordinary and high-performance cement paste

Analyzing the graphics it is easily seen that the effects of elevated temperatures on the trend of the curves of the two cement pastes is very similar, the differences residing in different losses of masses.
The difference between ordinary and high-performance cement paste lies in the different water/cement ratio. The ordinary cement paste has a W/C=0.6, higher than high-performance cement paste, that has W/C=0.3. This difference of water produces the different mass losses.
The weight loss in concrete during exposure to elevated temperatures can be related to the change in the mechanical properties of the concrete.
Also starting from 20°C there is a loss of mass due to evaporation of free water, that is completely eliminated at 120 ° C. The first endothermic peak observed at 120 °C indicates the dehydration of cement paste by driving out of physically bound water, with a mass loss 12.67% in the ordinary cement paste and 10.24% in the high-performance cement paste, with a difference of about 2%. On the other hand, the first endothermic peak at nearly 300°C indicates probable gas releases. The second endothermic peak observed at 480 °C is the calcium hydroxide $Ca(OH)_2$ that turns into CaO lime. The third endothermic peak at nearly 730°C can be the indicator for the second step of CSH gel dehydration. With increase of temperature take place a possible generation of a new phases due to such extremely high temperatures. The last endothermic peak is due to decomposition of $CaCO_3$.

b) Black limestone

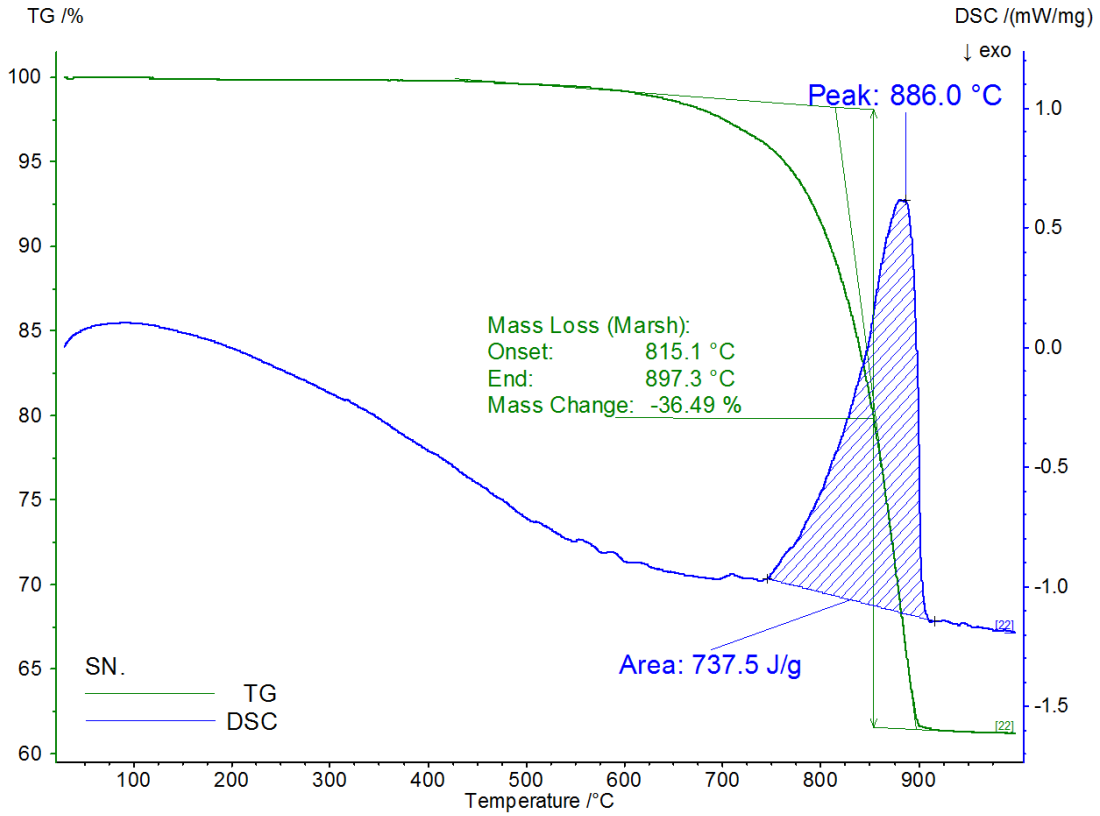

Figure 41: TGA/DSC black limestone sand

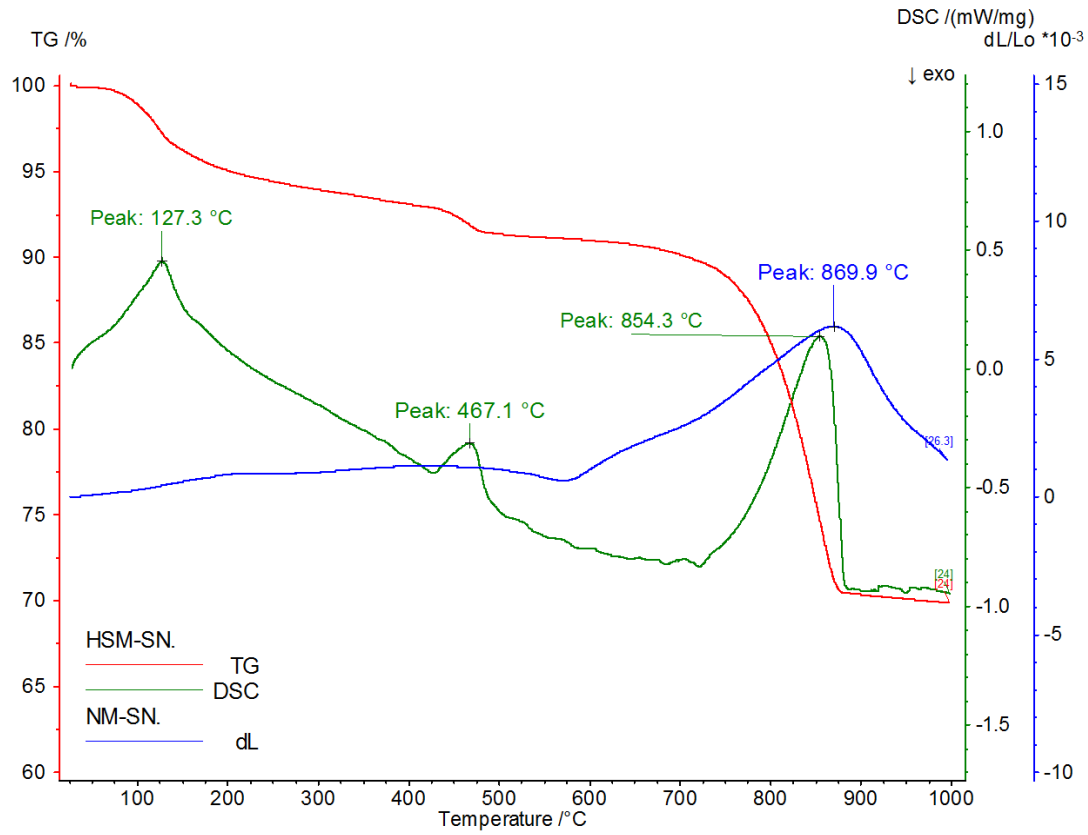

Figure 42: TGA/DSC high-performance black limestone mortar, DIL normal black limestone mortar

The curve of the black limestone aggregate shows a significant loss of mass, which begins around 800 ° C and ends at 900 ° C, this mass loss is due to the decarbonation reaction. The decarbonation consists in the decomposition of calcite $CaCO_3$ in CaO in according to following reaction:

$$CaCO_3 = CaO + CO_2$$

This chemical reaction is accompanied by a significant loss of mass due the enactment of the CO_2, the average loss is observed approximately 36.49%. The endothermic peak is realized at 886 °C.

Middle enthalpy variation obtained is 737.5 J/g. Black limestone mortar has the same characteristic of high-performance concrete, with the addition of the characteristic peak of the chemical reaction $CaCO_3$. Dilatometric analysis shows that the sand limestone dilates very little and is hampered by the contraction of the concrete around 600°C.

c) Granite

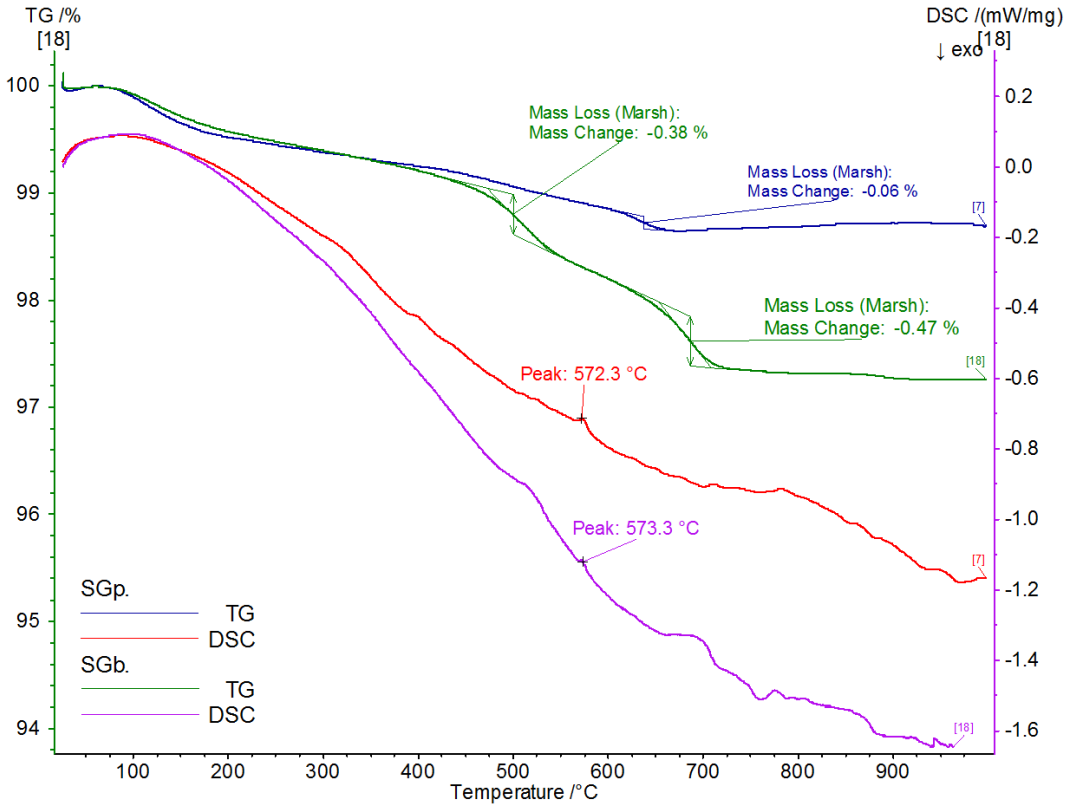

Figure 43: TGA/DSC granite sand black part and pink part

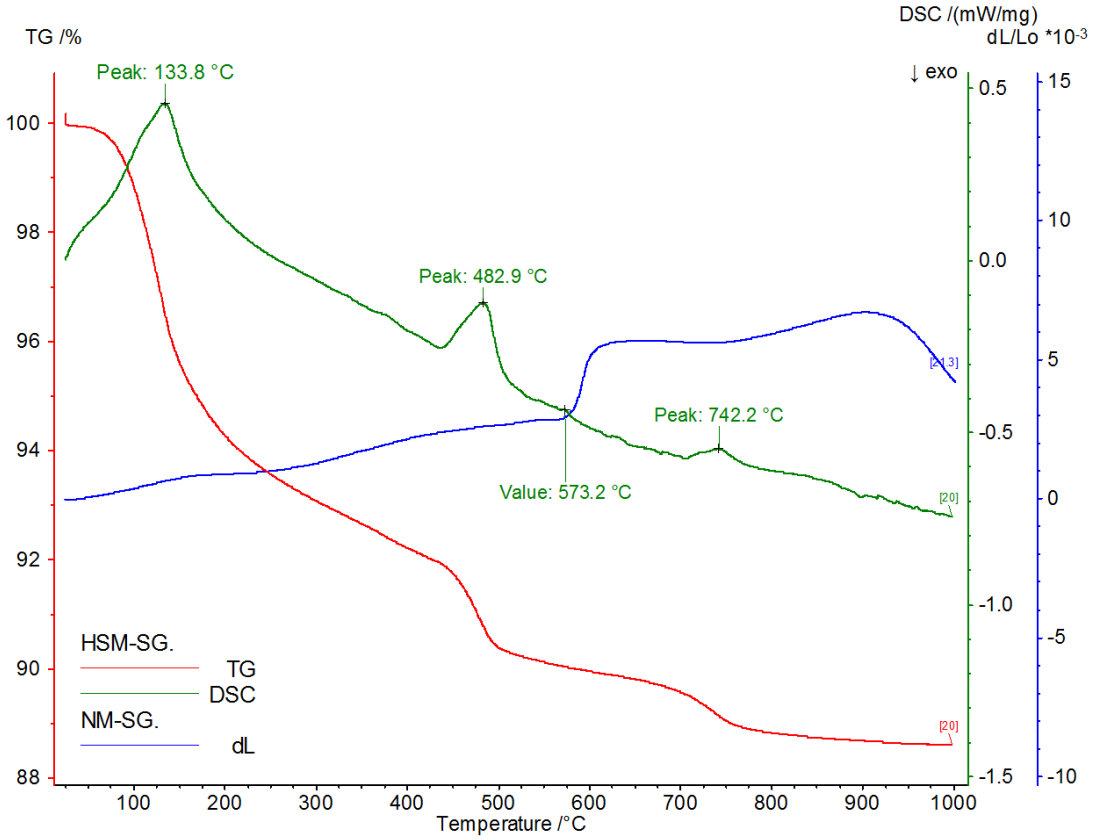

Figure 44: TGA/DSC high-performance granite mortar, DIL normal black granite mortar

Analyzing the loss of mass of the granite, you immediately notice as the most relevant is the loss of mass caused by the transformation of quartz from α to β 573 ° C, this mass loss is of 0.06%.
The transformation of the quartz is visible in DSC aggregate, DSC mortar and Dilatometry.
The mortar, in addition to the peak of the transformation of quartz also presents the other characteristic peaks of the high-performance concrete.
Micas component was separated from the granite and examined. Analyzing results, you may notice a loss of mass in two steps due to dehydration of chlorite , the first loss is recorded around 400 ° C to 500 ° C and is due to dehydration between the sheets, the second mass loss is due to dehydration of the sheets. The total mass lost in this temperature range is of 0.85%, this mass loss is due to micas structure, which presents itself as a set of sheets with bound water inside.

d) Flint

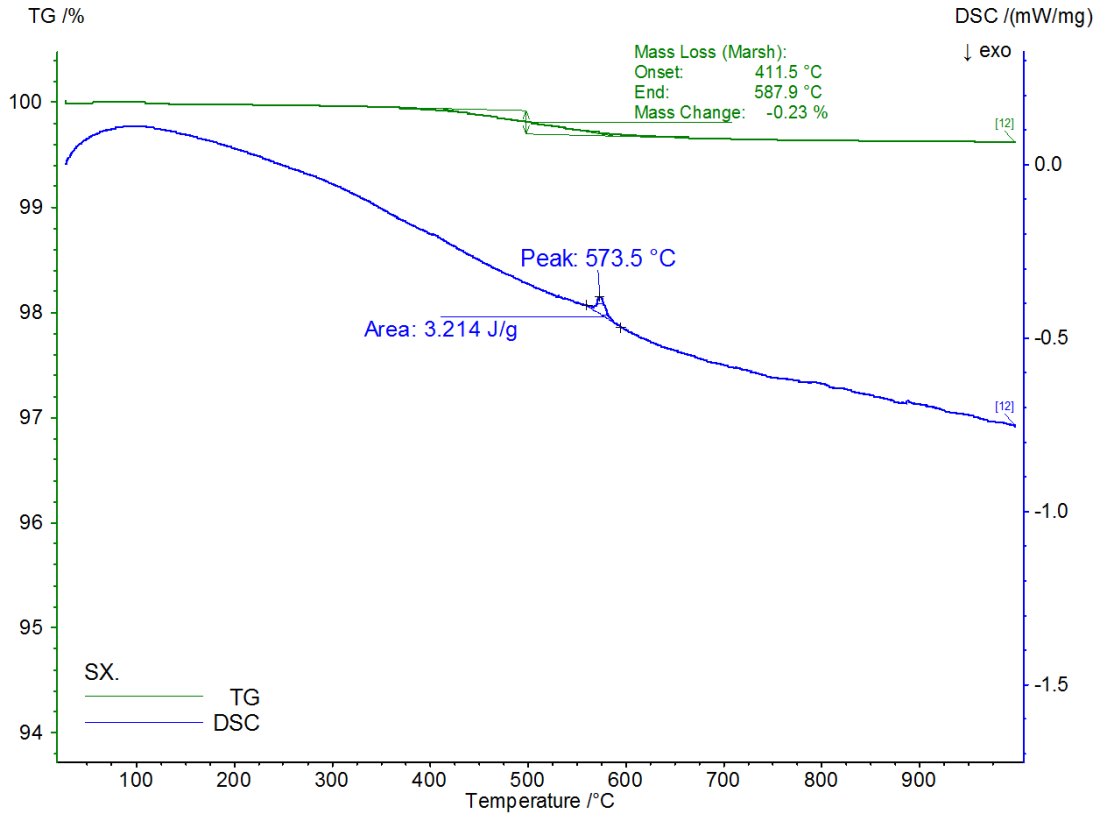

Figure 45: TGA/DSC flint sand

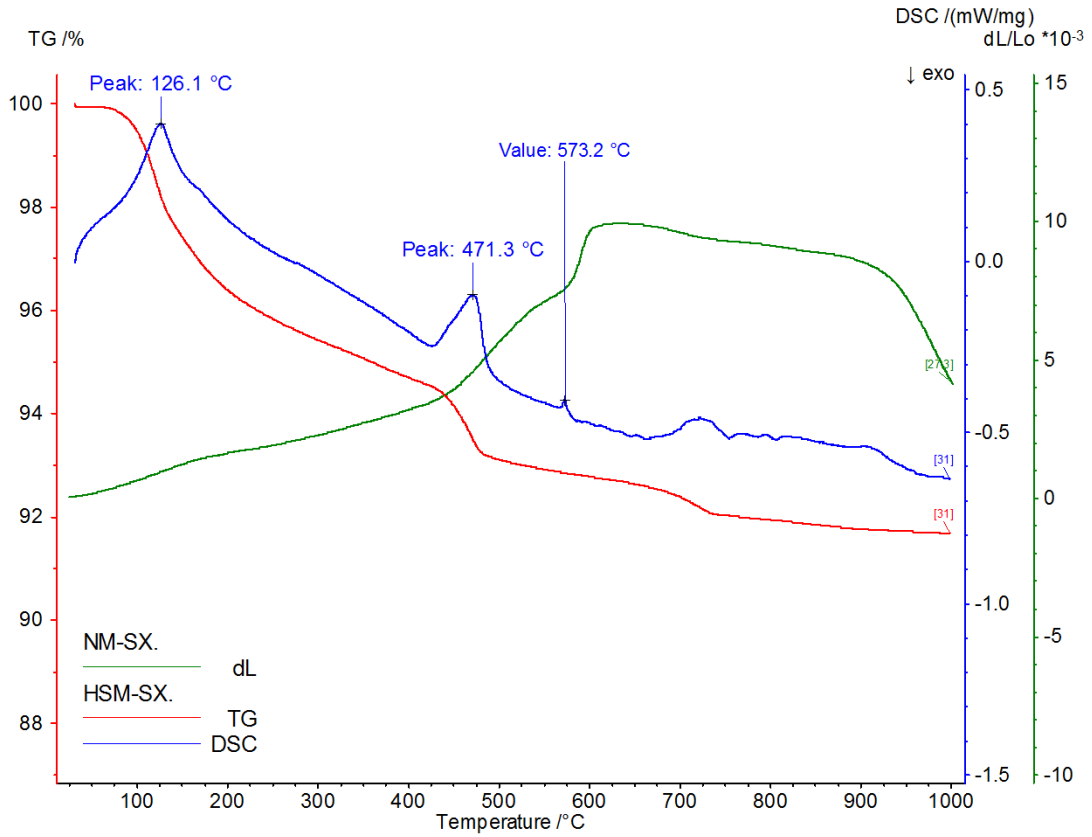

Figure 46: TGA/DSC high-performance flint mortar, DIL normal flint mortar

Flint aggregates contains quartz, as granite is subjected to transformation from α to β, with a loss of mass approx. 0.20%. This transformation in the natural sand caused a slight volume expansion above 550 °C.
Analyzing flint mortar curve, you can also notice the peaks due to the presence of the cement.

Conclusions

Concrete material in structures is likely exposed to high temperatures during fire. The relative proprieties of concrete after such an exposure are of great importance of terms of serviceability of buildings. This work presents the effects of elevated temperatures on the physical proprieties of three different mortars mixtures prepared by black limestone sand, granite sand and flint sand.

Test samples are subjected to elevated temperatures ranging from 20°C to 1000°C with dilatometry and ATG/DSC test. After exposure, weight losses are determined. Test results indicated that weight of the specimen significantly reduced with an increase on temperature.

When exposed to high temperature the chemical composition and physical structure of cement paste change considerably. The value of the mass loss is dependent on the water cement ratio, a high ratio produces a high mass loss. Ordinary cement paste with W/C = 0.6 lose more than the high-performance cement paste, that has W/C=0.3. The dehydration due to the release of chemically bound water from the calcium silicate hydrate CSH becomes significant above about 110°C. The dehydration of the hydrated calcium silicate and the thermal expansion of the aggregate increase internal stressed and from 300°C micro cracks are induced through the material. Calcium hydroxide $Ca(OH)_2$, which is one of the most important compounds in cement paste, dissociates at around 530°C resulting in the shrinkage of concrete. CSH gel, which is the strength giving compound of cement paste, decomposes further above 600°C. At 800°C is usually crumbled and above 1150°C feldspar melts and the other minerals of cement paste turn into a glass phase. As a result, severe microstructural changes are induced and concrete loses its strength and durability.

All three mortars exhibit the same behavior described for cement paste, but the strength degradations of concretes with different sands are not the same under high temperatures. This is attributed to the mineral structure of the aggregates. Quartz in siliceous aggregates polymorphically changes at 573°C with a volume expansion and consequent damage. Flint sand containing more quantities of SiO_2 than granite sand, their behavior is similar with a difference in expansion. Black limestone sand behaves in a totally different way, $CaCO_3$ turns into CaO at 800-900°C, and expands with temperature. Shrinkage may also start due to the composition of $CaCO_3$ into CO_2 and CaO with volume changes causing destructions.

Limestone sand dilates very little and is overwhelmed by the contraction of the cement paste when subjected to high temperatures. The granite sand is constituted by micas, the structure of which influences the characteristics of the sand subjected to high temperatures.

It is possible to consider the thermal expansion coefficient as linear for the low temperatures.

The most important that is pointed out in this variations is the mineralogical composition.

Finally, when comparing the different mineralogical natures, no conclusive remark can be formulated except that siliceous aggregates seems to dilate a little more at the lower temperatures than calcareous aggregates.

However, the tests done with the three different sands, using a similar cement paste mix show that the different sands have a significant influence on the behavior of mortars at high temperatures.

References

Arioz O. *Effects of elevated temperatures on properties of concrete.* Fire safety journal 42 (2007) 516-522;

Bazant Z. P. *Delayed thermal dilatations of cement paste and concrete due to mass transport.* Nuclear engineering and design 14 (1970) 308-318.

Bazant Z.P., Kaplan M.F., Haslach H. *Concrete at high temperatures: material properties and mathematical models.* Applied mechanics reviews 50 (1997) B75-B75.

Ghanem H., Zollinger D., Lytton R., Ghanem N. D*etermining ASR characteristics using dilatometer method.* Construction and building materials 36 (2012) 1008-1015.

Kong D., Sanjayan J. G. *Damage behavior of geopolymer composites exposed to elevated temperatures.* Cement & concrete composites 30 (2008) 986-991.

Kong D., Sanjayan J. G. *Effect of elevated temperatures on geopolymer paste, mortar and concrete.* Cement and concrete research 40 (2010) 334-339.

Luccioni B. M., Figueroa M. I., Danesi R. F. *Thermo-mechanic model for concrete exposed t elevated temperatures.* Engineering structures 25 (2003) 729-742.

Mashall A. L. *The thermal properties of concrete.* Civil engineering department, Sunderland Polytechnic (1972).

Mukhopadhyay A. K., Zollinger D.G. *Development of dilatometer test method to measure coefficient of thermal expansion of aggregates.* Journal of materials in civil engineering 21 (2009) 781-788.

NF EN 932-1 (1996). *Essais pour déterminer les propriétés générales des granulats.*

NF EN 933-2 (1996). *Essais pour déterminer les caractéristiques géométriques des granulats.*

NF EN 1936 (2007). *Détermination des masses volumiques réelle et apparente et des porosités ouverte et totale.*

NF P 94-056 (1996). *Analyse granulométrique.*

NF P 94-057 (1992). *Analyse granulométrique des sols.*

Niry Razafinjato R. *Etude pétrographique et de stabilité thermique des granulats.* (2012) Rapport de stage, Université de Cergy-Pontoise, Neuville-sur-Oise, France.

Niry Razafinjato R., Beaucour A.-L., Hebert R., Noumowé A., Ledésert B. & Bodet R. (2013). *Thermal stability of different siliceous and calcareous aggregates subjected to high*

temperature. Paper presented at the RILEM 3rd international workshop: concrete spalling due to fire exposure, Paris, France.

Niry Razafinjato R., Beaucour A.-L., Hebert R., Noumowé A., Ledésert B. & Bodet R. (2014). *Comportement à haute température des bétons de granulats naturels siliceux et calcaires.* Paper presented at the 32rd international workshop: concrete spalling due to fire exposure, Paris, France.

Niry Razafinjato R., Beaucour A.-L., Hebert R., Noumowé A., Ledésert B. & Bodet R. (2014). *Comportement à haute température des granulats naturels siliceux et calcaires et leur influence sur celui du béton.* (2012) Université de Cergy-Pontoise, Neuville-sur-Oise, France.

Peeters P.J.M., de Borts R. (*Analysis of concrete structures under thermal loading.* Computer methods in applied mechanics and engineering 77 (1989) 293-310.

Robert F., Colina H. *The influence of aggregates on the mechanical characteristics of concrete exposed to fire.* Magazine of concrete research 61 (2009) 311-321.

Schneider U. *Concrete at high temperatures.* University of Kassel, Mönchebergstr, fire safety Journal 13 (1988) 55-68.

Schrefler B.A., Pesavento F., Gawin D. *Modelling of hygro-thermal behaviour of concrete at high temperature with thermo-mechanical and mechanical material degradation. (2002)* University of Padua, Padua, Italy.

Schreyer H.L., Yazdani S. A*n anisotropic damage model with dilatation for concrete.* (1988) University of New Mexico, Albuquerque, USA.

Uygunoglu T., Bekir T. *thermal expansion of self-consolidating normal and lightweight aggregate concrete at elevated temperature.* Construction and building materials 23 (2009) 3063-3069.

Xing Z. I*nfluence de la nature minéralogique des granulats sur leur comportement et celui du béton à haute température.* (2011) These de doctorat, Université de Cergy-Pontoise, Neuville-sur-Oise, France.